

Structure Functions at HERA

Elisabetta Gallo, INFN Firenze

On behalf of

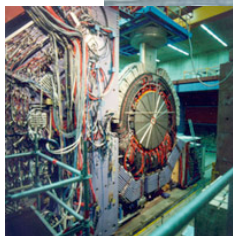


- o HERA and structure functions
- o Low Q^2 data (F_2)
- o High Q^2 results (CC, NC, $\times F_3$)
- o Combined data
- o Parton densities functions (PDFs)
- o Polarization
- o Low energy run results (F_L)

Zeuthen, 3/12/2008

HERA (1992-2007)

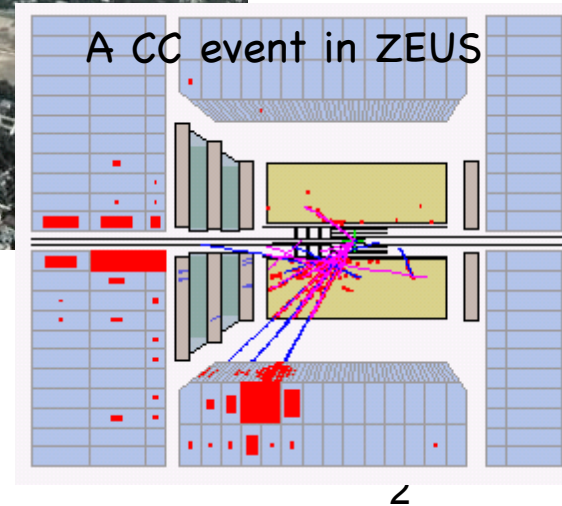
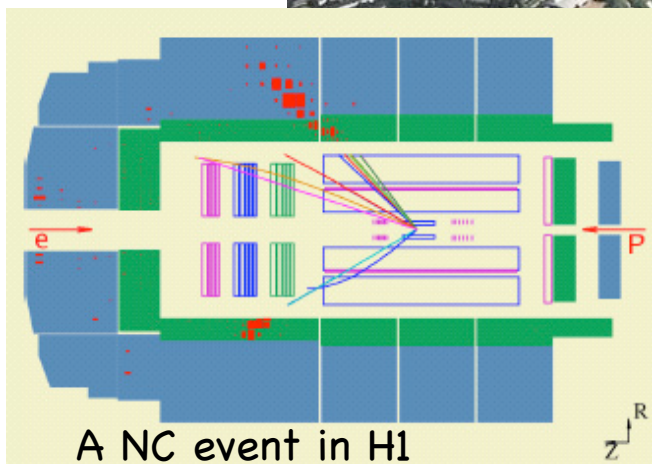
H1



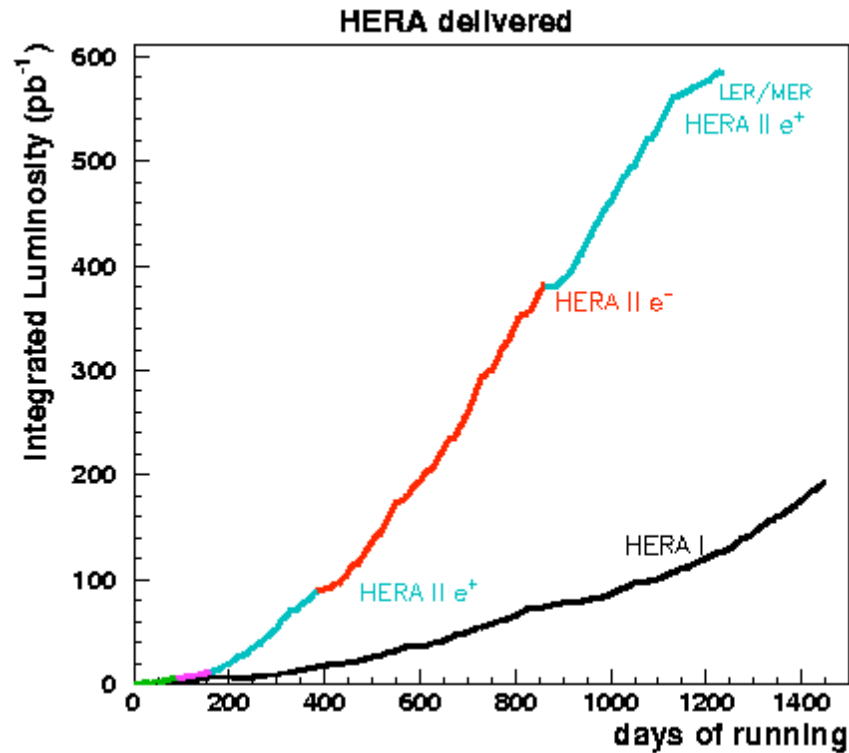
ZEUS



HERA: 318 GeV
p (920 GeV) e (27.6 GeV)

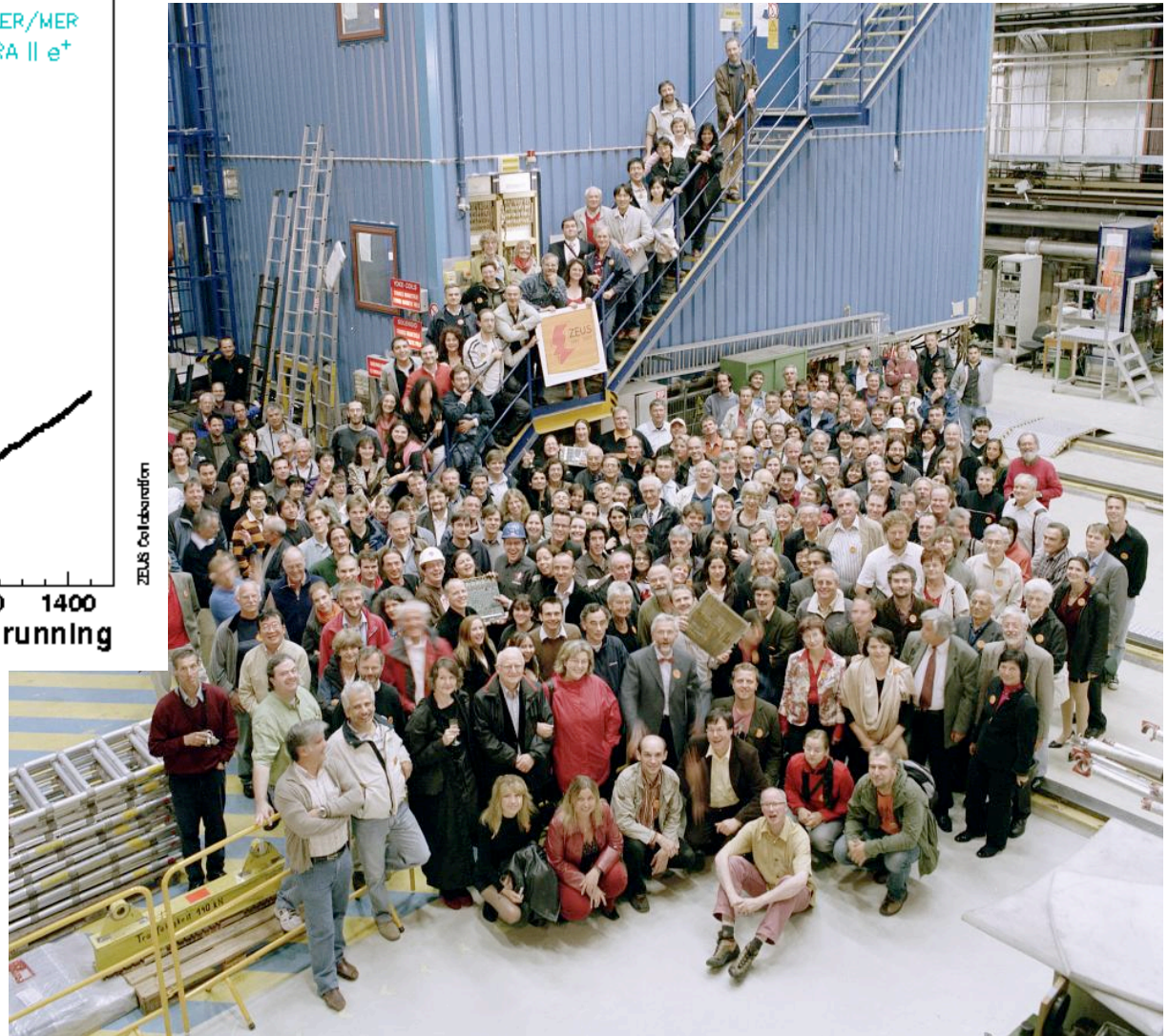


HERA luminosity

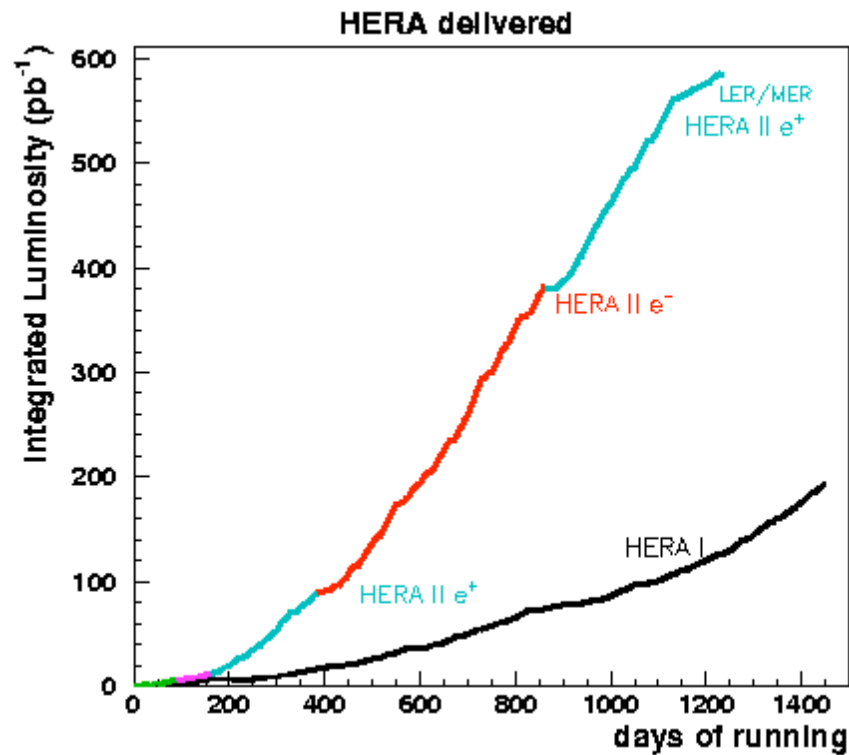


Last Fill 30/6/2007,

0.5 fb^{-1} per exp., 1 fb^{-1}
H1+ZEUS combined, \sim equal
luminosity for e^+p, e^-p and
LH, RH polarisations.



HERA luminosity

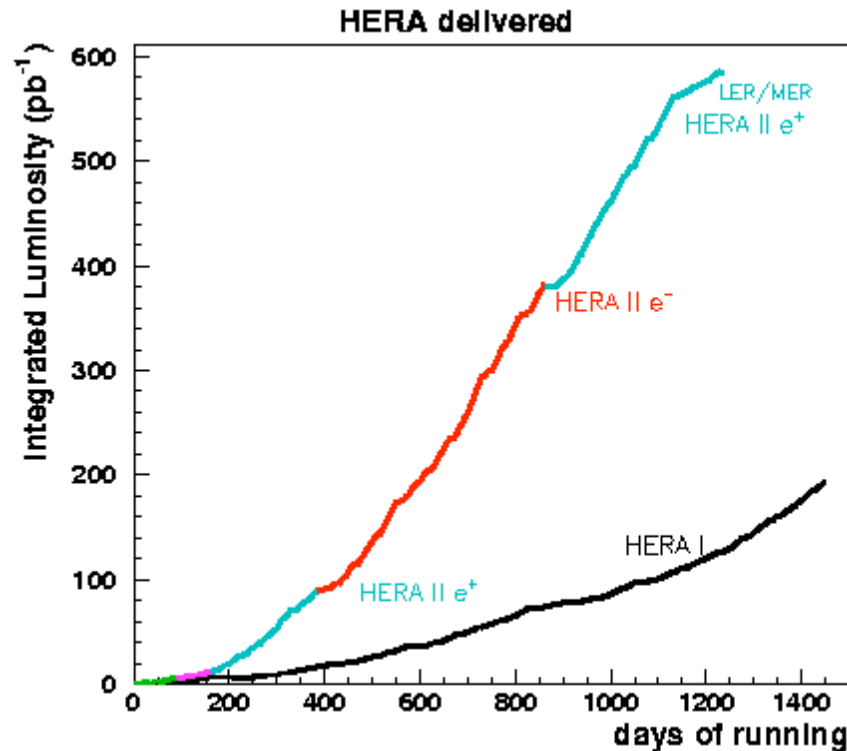


Last Fill 30/6/2007,

0.5 fb^{-1} per exp., 1 fb^{-1}

H1+ZEUS combined

HERA luminosity



Last Fill 30/6/2007,

0.5 fb^{-1} per exp., 1 fb^{-1}

H1+ZEUS combined

Both detectors dismantled, excellent work of the DESY technicians and technical coordinators!

HERA kinematics

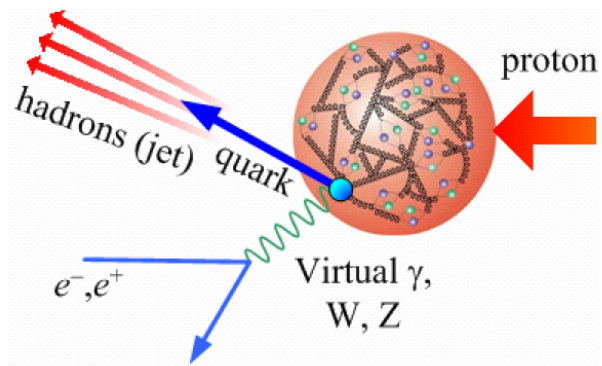
$$Q^2 = -q^2$$

$$x$$

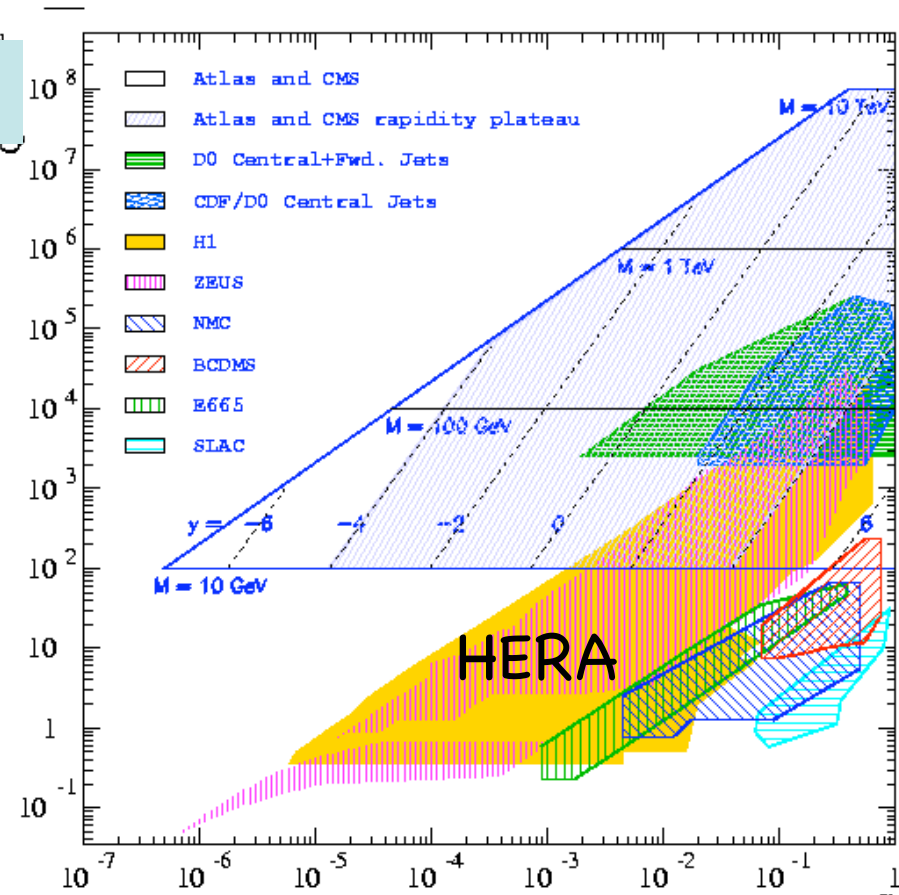
$$y$$

$$Q^2 = sxy$$

virtuality of γ^*, Z
 Bjorken x
 inelasticity



Q^2



HERA

x Bjorken

$$\sigma_r^\pm = \frac{d^2\sigma^\pm}{dx dQ^2} \frac{Q^4 x}{2\pi\alpha^2 Y_+} = \tilde{F}_2^\pm \mp \frac{Y_-}{Y_+} x \tilde{F}_3^\pm - \frac{y^2}{Y_+} \tilde{F}_L^\pm$$

At high Q^2

At high y

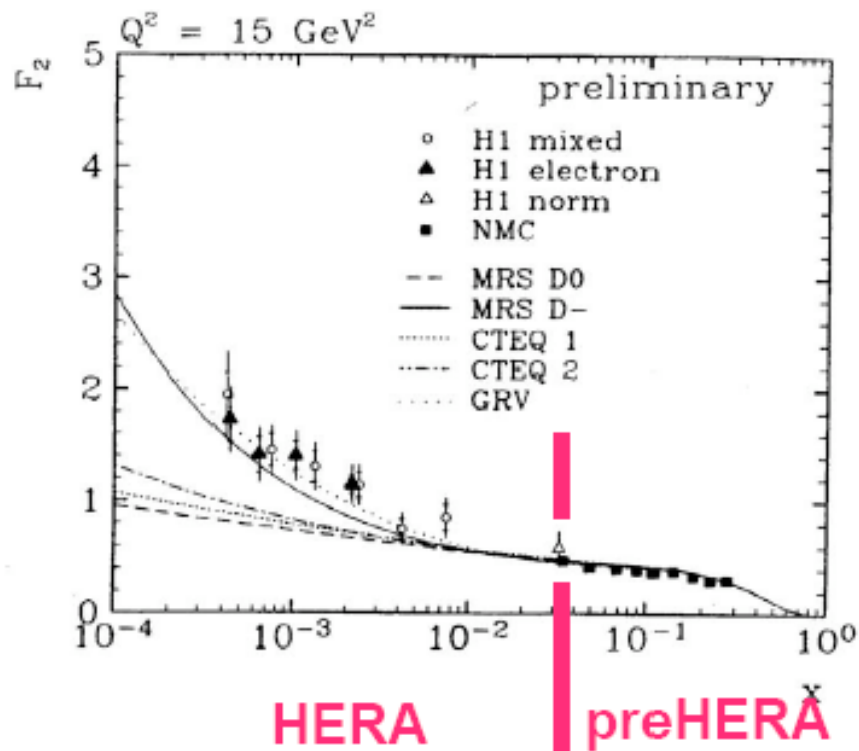
Main structure function

Low Q^2 F_2 measurements

Measurement of F_2 at low x, Q^2

First F_2 from HERA ,
Durham Workshop 1993

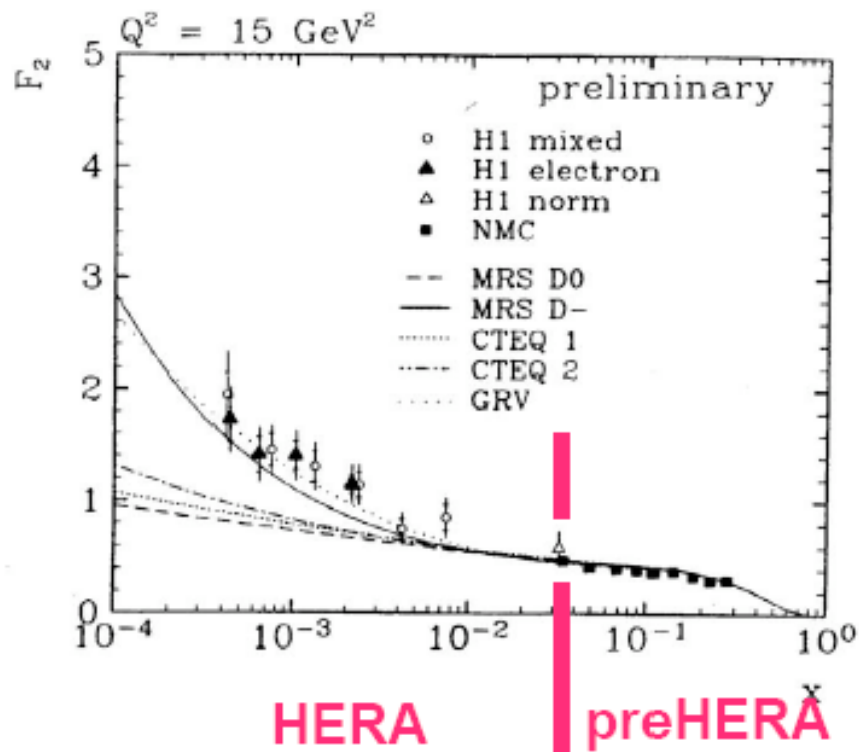
Since then, quite a lot of
developments:



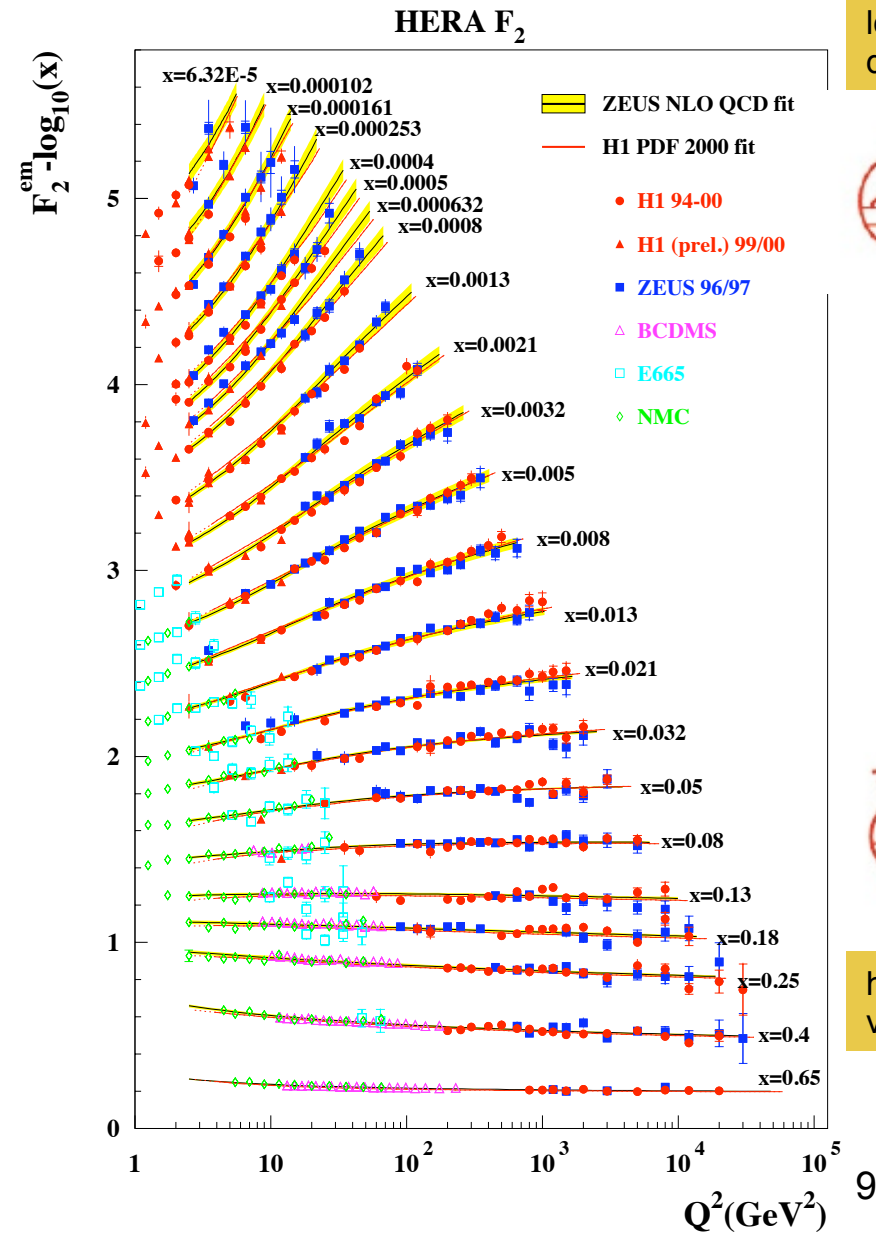
- very precise data on a wide kinematic range
- PDFs from global fits and HERA fits
- F_2 from charm and beauty
- combined H1+ZEUS data and PDFs

Measurement of F_2 at low x, Q^2

First F_2 from HERA
Durham Workshop 1993



$$F_2 = x \sum e_q^2 (q + \bar{q})$$



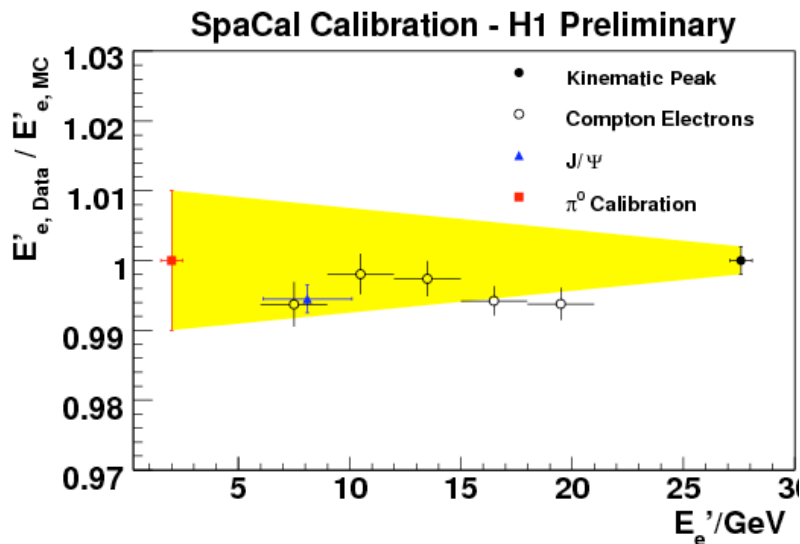
low x , sea dominated



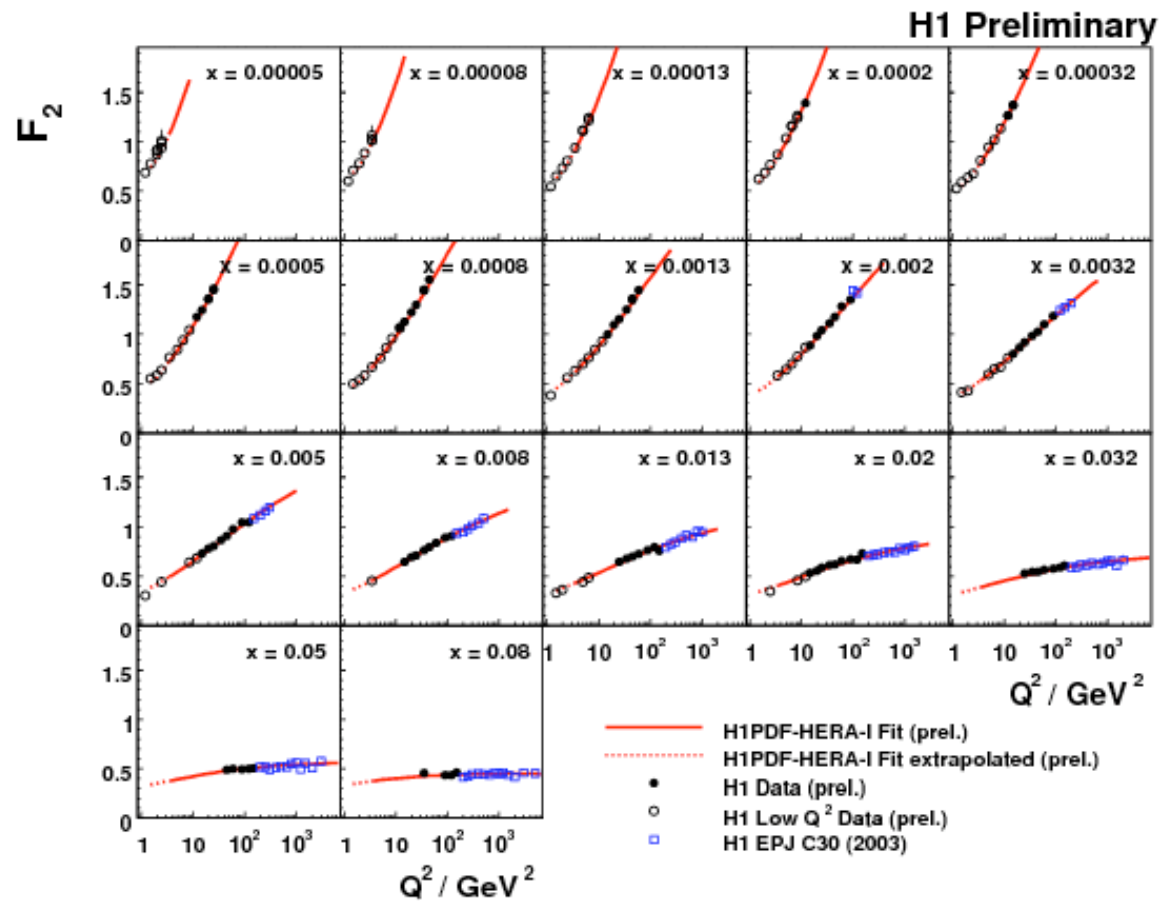
high x , valence q

Latest H1 measurement

New 2000 data



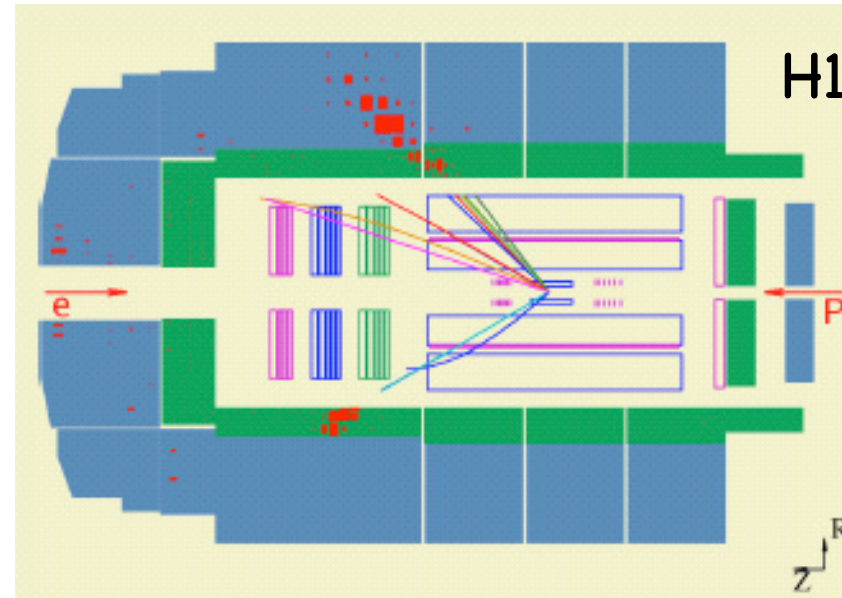
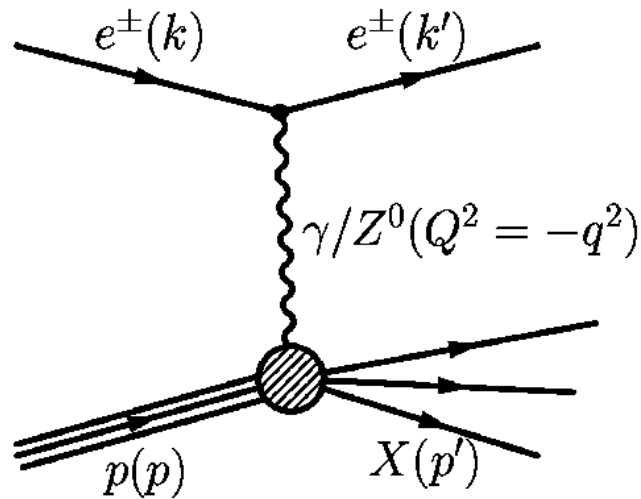
2000 data added, most accurate measurement in the kinematic region $12 < Q^2 < 150 \text{ GeV}^2$, $0.0002 < x < 0.1$, 1.5-2% syst. error



High Q^2 measurements

Neutral Current at high Q^2

$$\sigma(e^\pm) \propto Y_+ F_2 \mp Y_- x F_3$$



$$F_2^{L,R} = \sum_q [xq(x, Q^2) + x\bar{q}(x, Q^2)] \cdot A_q^{L,R},$$

$$xF_3^{L,R} = \sum_q [xq(x, Q^2) - x\bar{q}(x, Q^2)] \cdot B_q^{L,R}.$$

γ

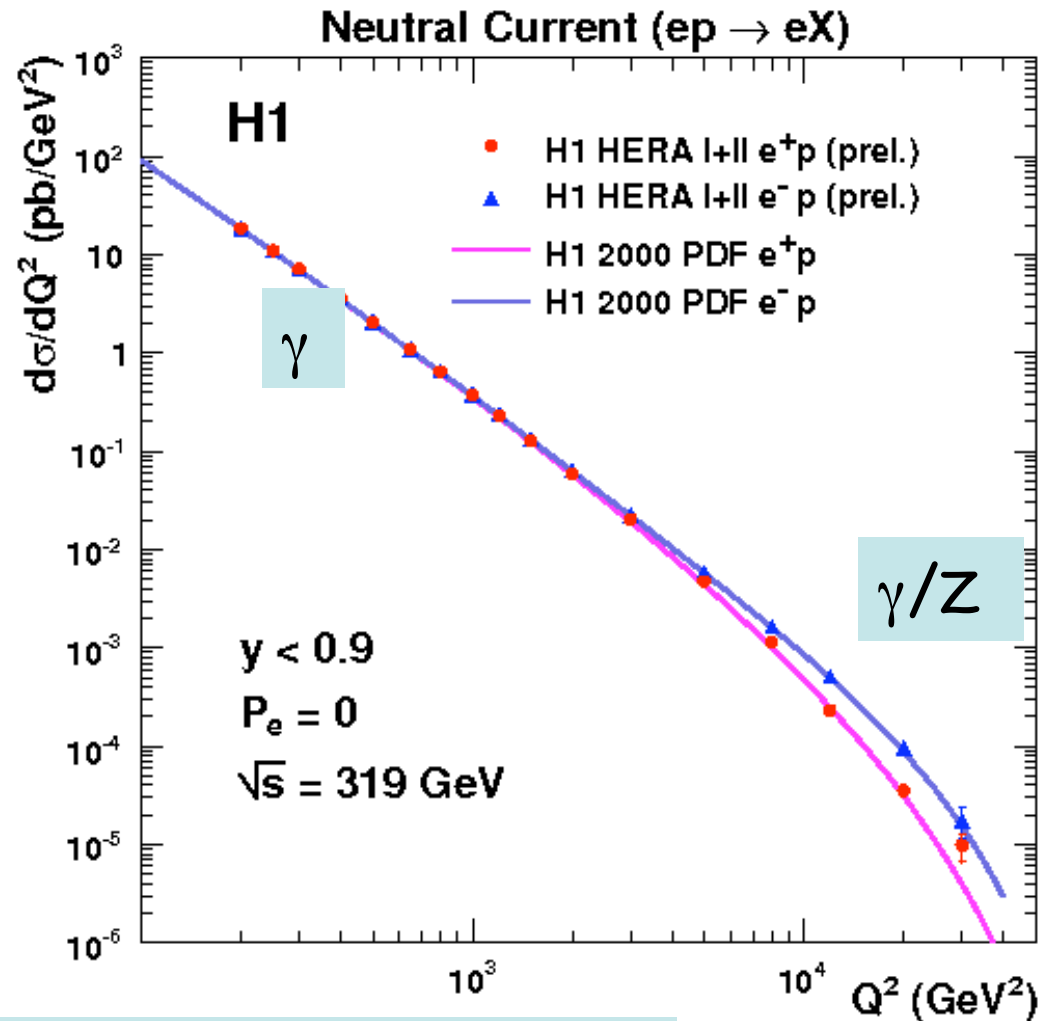
γ/Z

pure Z

$$A_q^{L,R} = Q_q^2 + 2Q_e Q_q (v_e \pm a_e) v_q \chi Z + (v_e \pm a_e)^2 (v_q^2 + a_q^2) (\chi Z)^2,$$

$$B_q^{L,R} = \pm 2Q_e Q_q (v_e \pm a_e) a_q \chi Z \pm 2(v_e \pm a_e)^2 v_q a_q (\chi Z)^2,$$

Q^2 dependence in NC

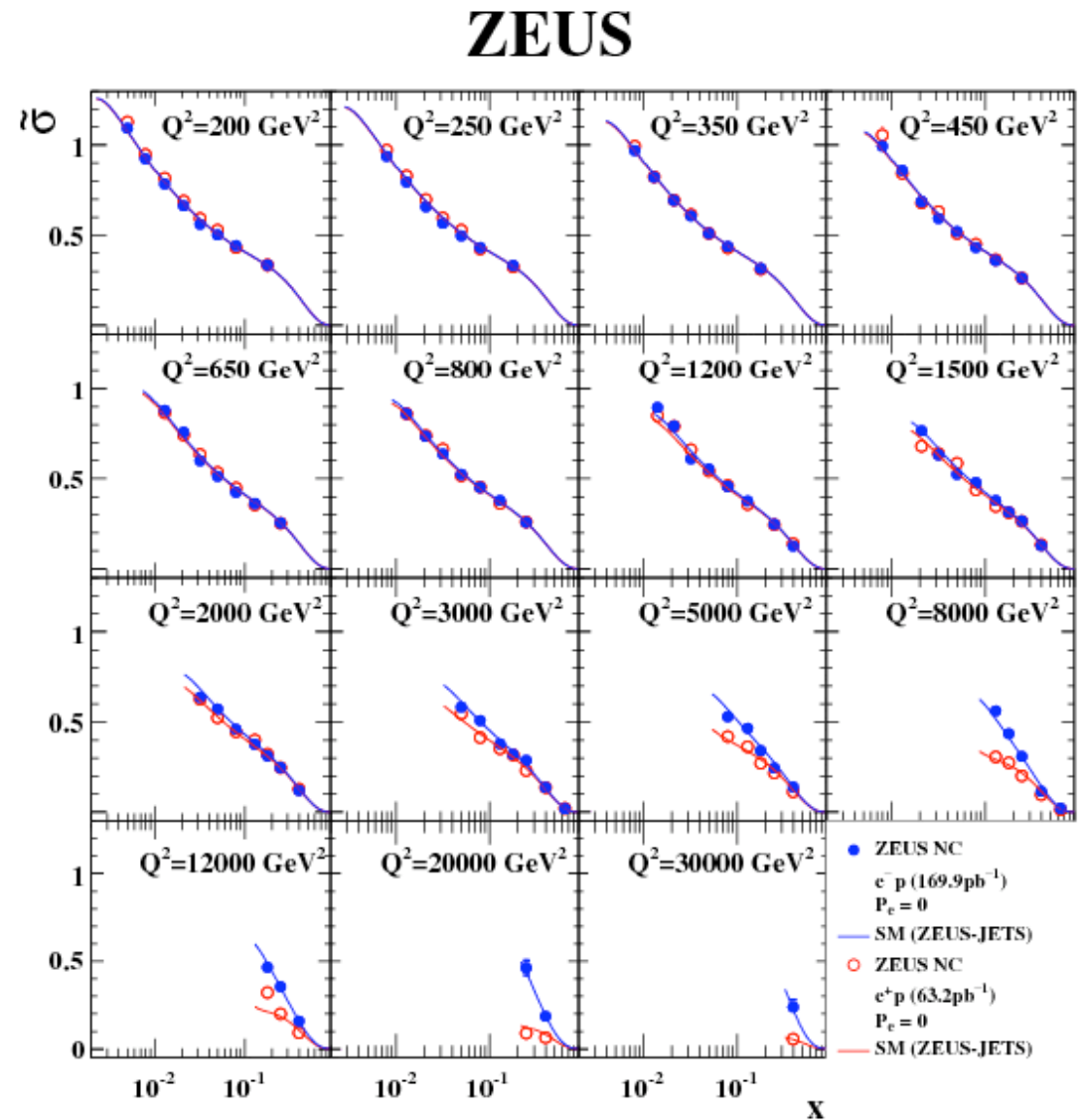
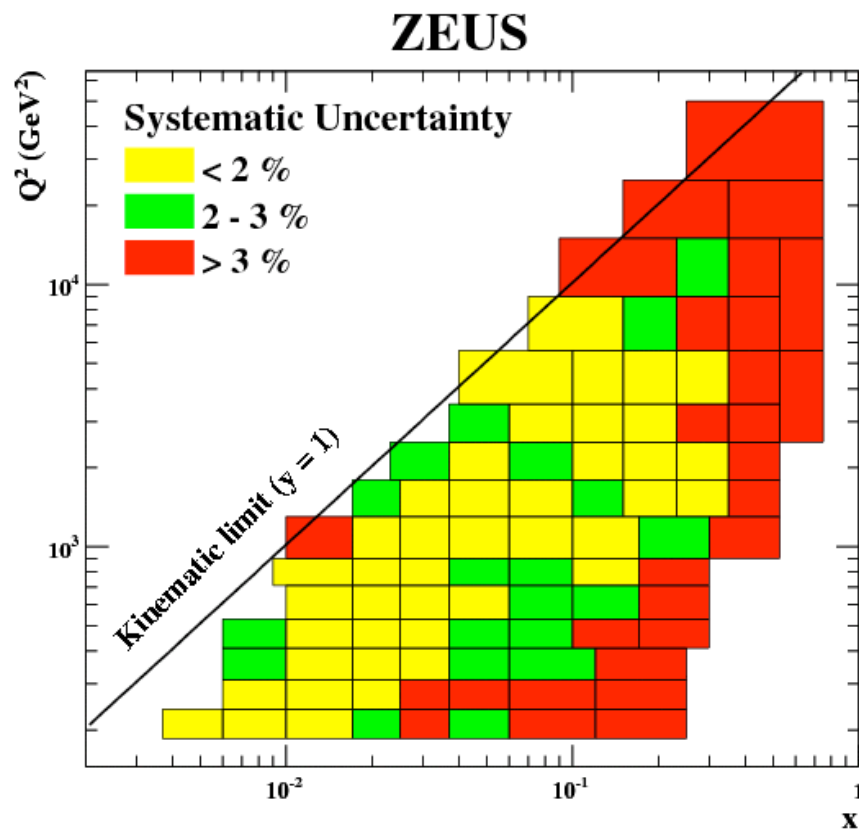


Contribution of interference and xF_3 only at very high Q^2

Good agreement with SM (EW+QCD) over 7 orders of magnitude

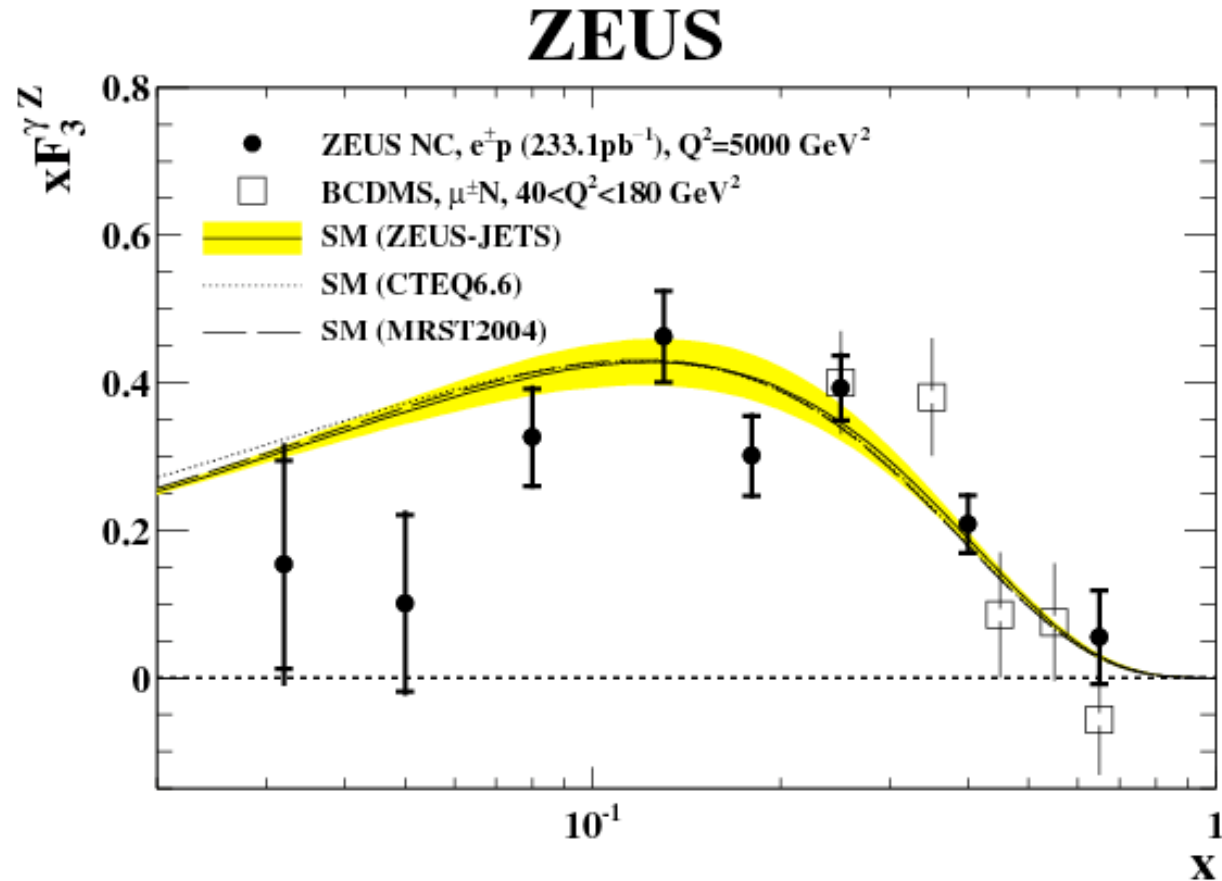
$x F_3$ and in NC

Latest paper on 2005 e-p data



xF_3 and in NC

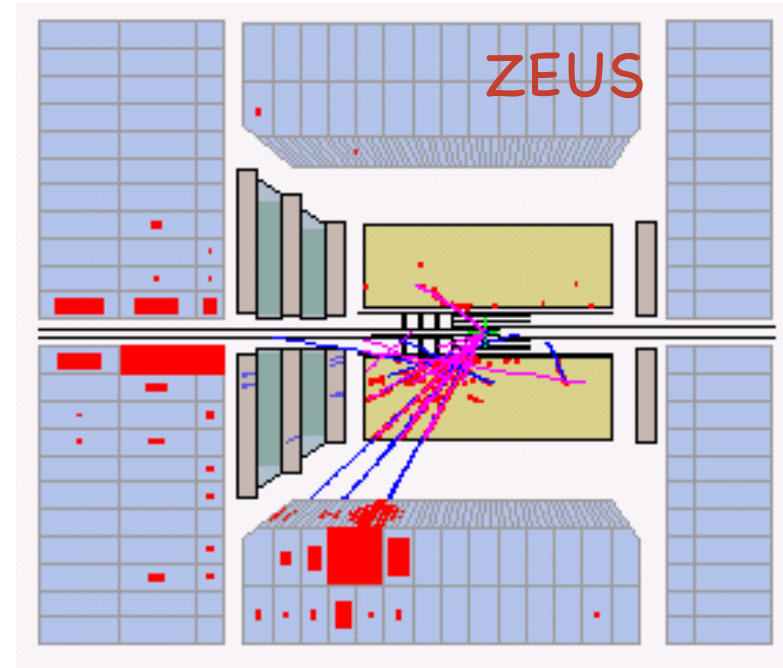
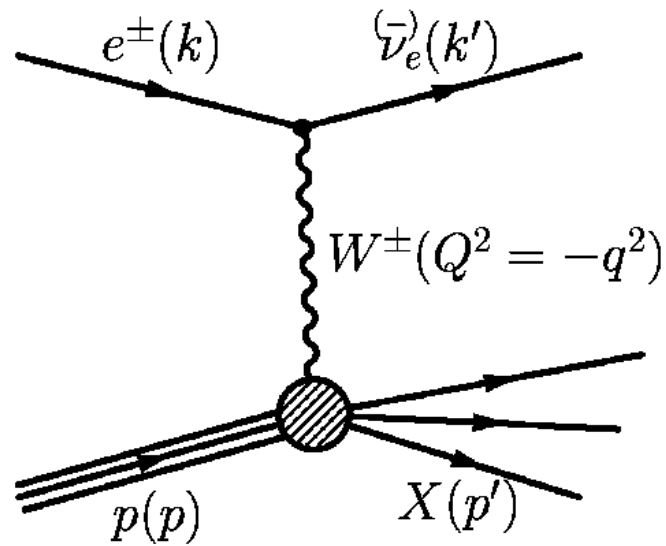
$$\sigma(e^\pm) \propto Y_+ F_2 \mp Y_- xF_3$$



Gives a measure of the u and d valence at low x

$$xF_3^{\gamma Z} = \frac{x}{3} (2u_v + d_v + \Delta)$$

Charged Current at high Q^2

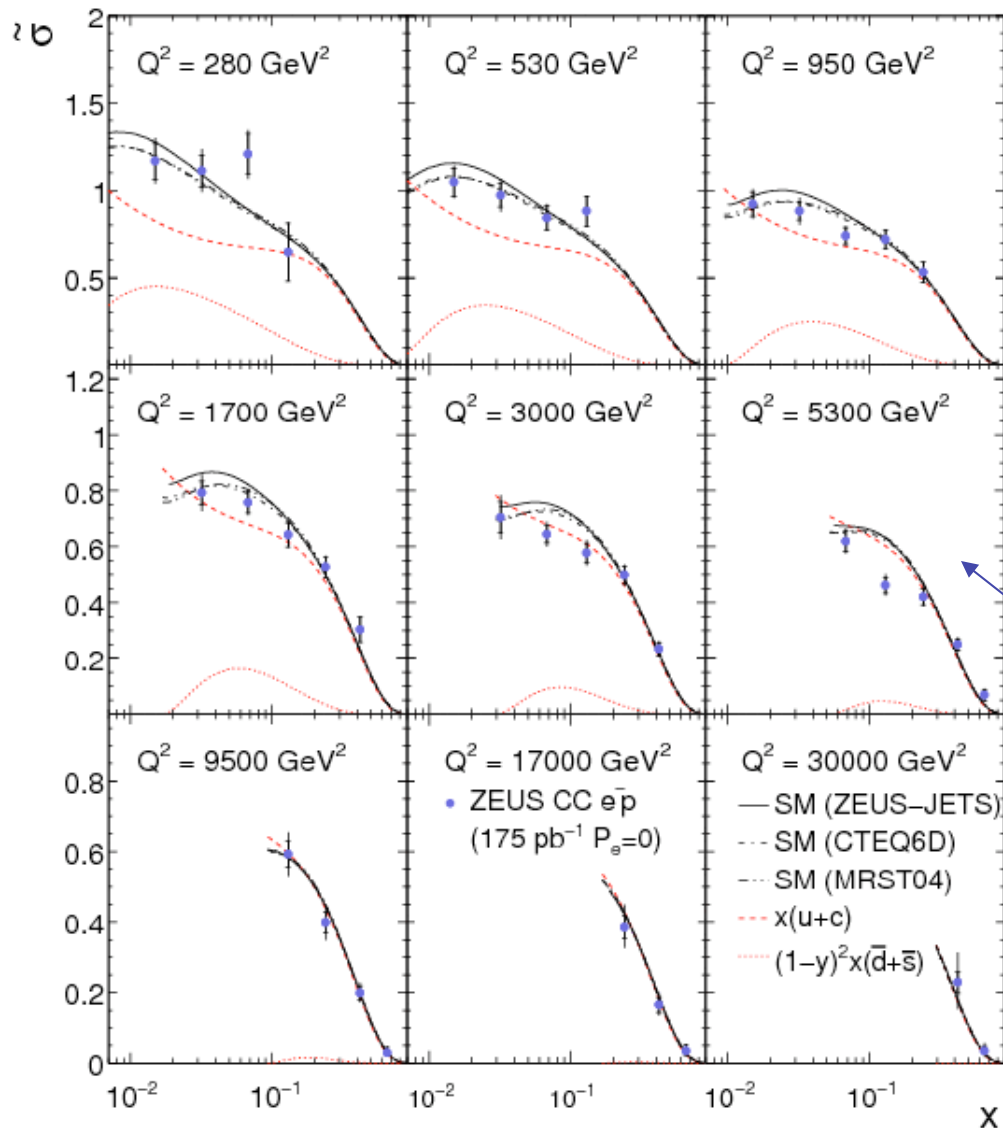


$$\frac{d\sigma_{unpolCC}^{e^+p}}{dQ^2 dx} = \frac{G_F}{2\pi} \cdot \left(\frac{M_W^2}{M_W^2 + Q^2} \right)^2 \left[\bar{u}_i(Q^2, x) + (1-y)^2 d_i(Q^2, x) \right]$$

$$\frac{d\sigma_{unpolCC}^{e^-p}}{dQ^2 dx} = \frac{G_F}{2\pi} \cdot \left(\frac{M_W^2}{M_W^2 + Q^2} \right)^2 \left[u_i(Q^2, x) + (1-y)^2 \bar{d}_i(Q^2, x) \right]$$

Differential CC cross-sections

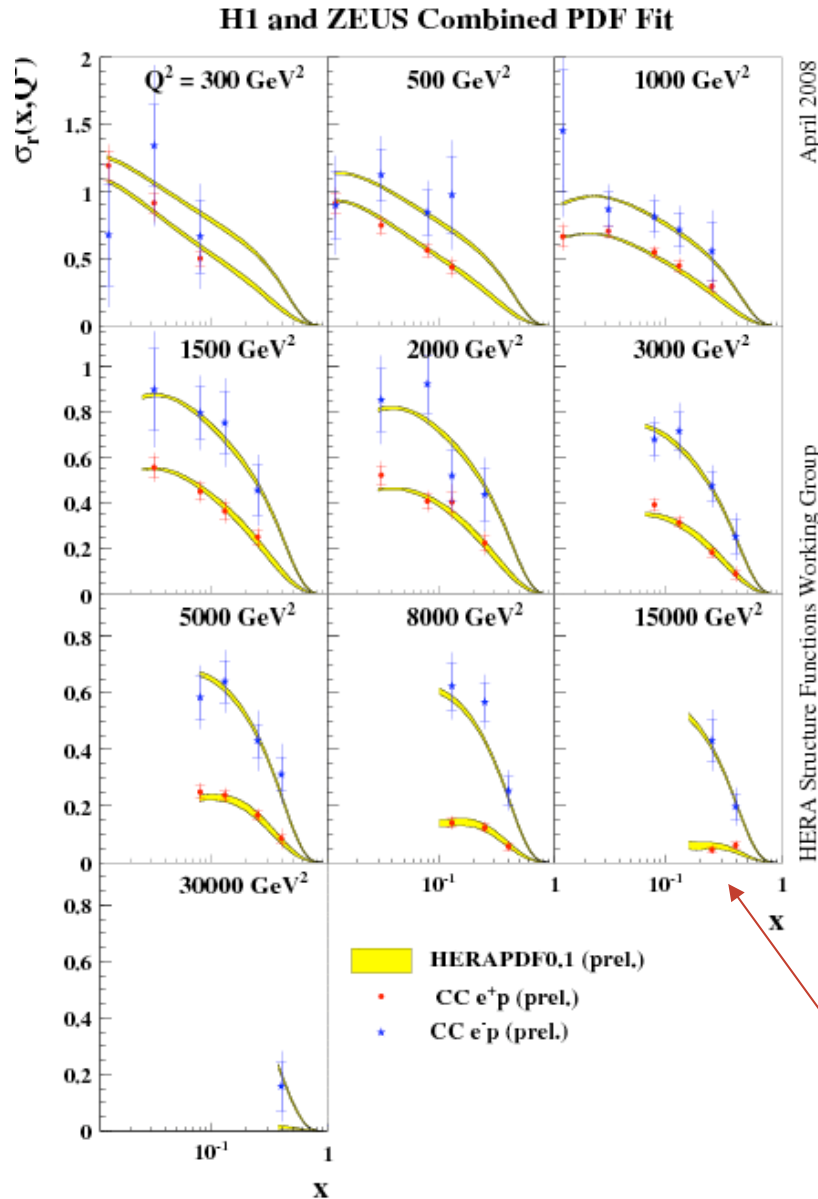
ZEUS



Differential CC cross sections can give information on the parton densities

e^-p u
dominated

Differential CC cross-sections



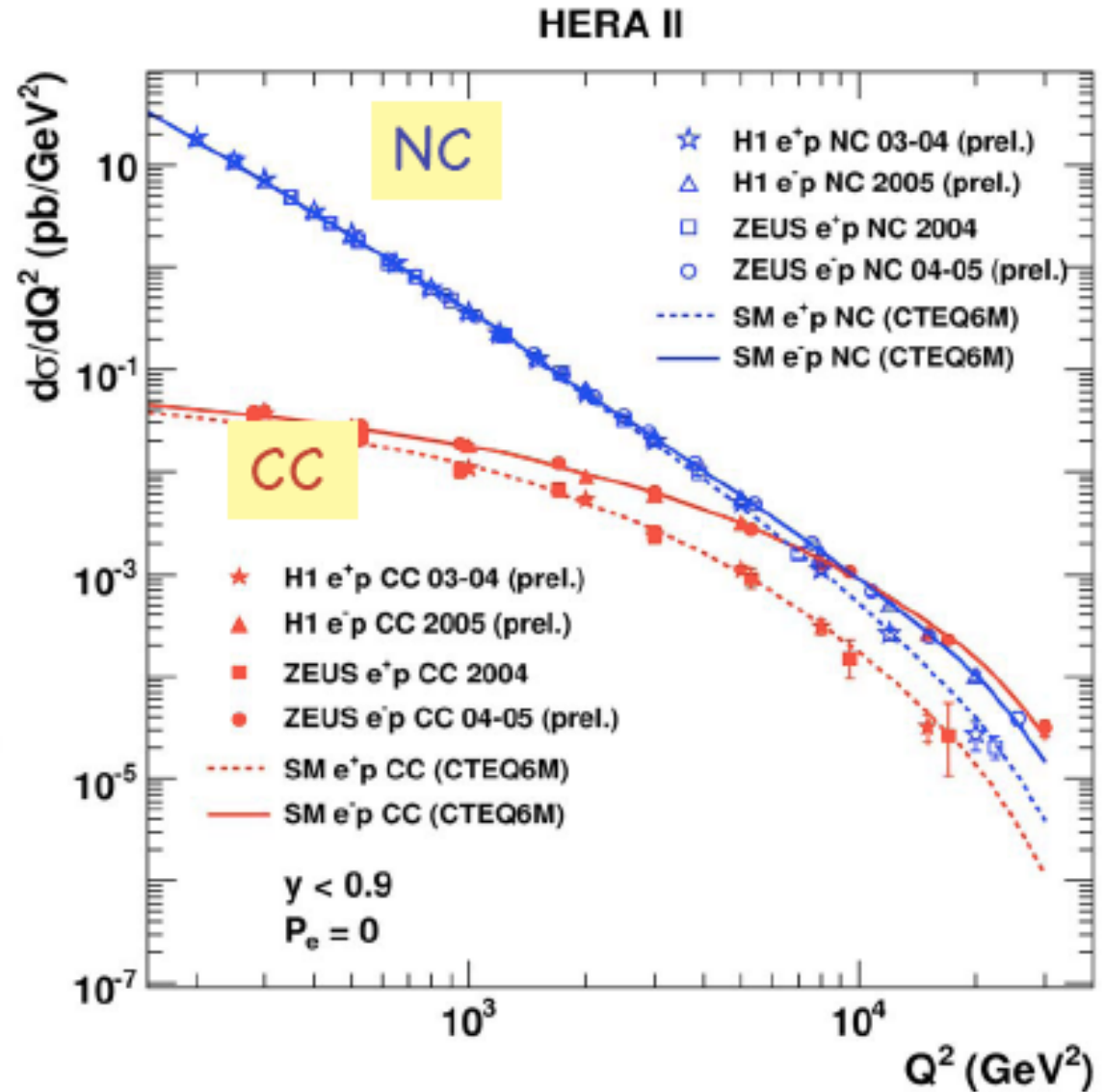
Differential CC cross sections gives information on the parton density flavours

e⁻p u dominated

e⁺p d dominated

NC/CC at high Q^2

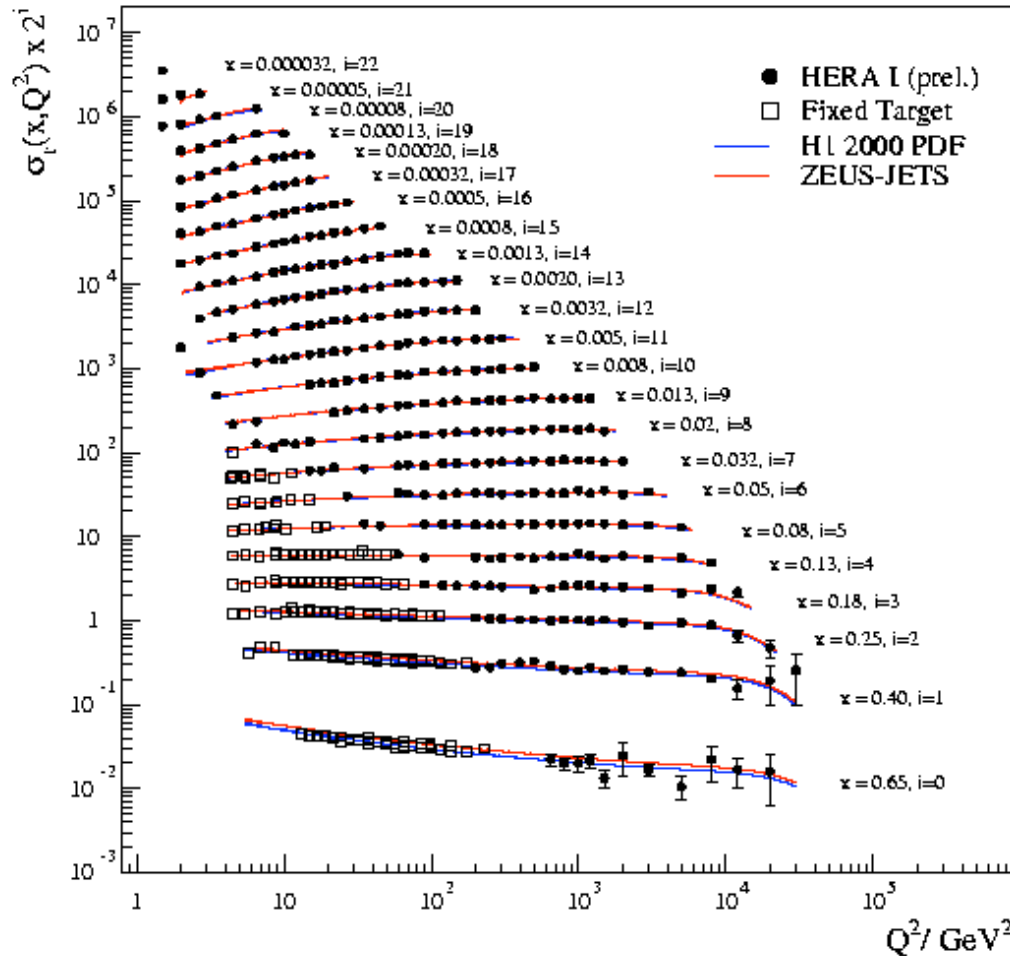
Textbook plot, the NC (EW) and CC interaction (pure weak) are of the same strength at the mass of the Z or W squared.



Combined H1+ZEUS data

Combined HERA I data

HERA I e^+p Neutral Current Scattering - H1 and ZEUS



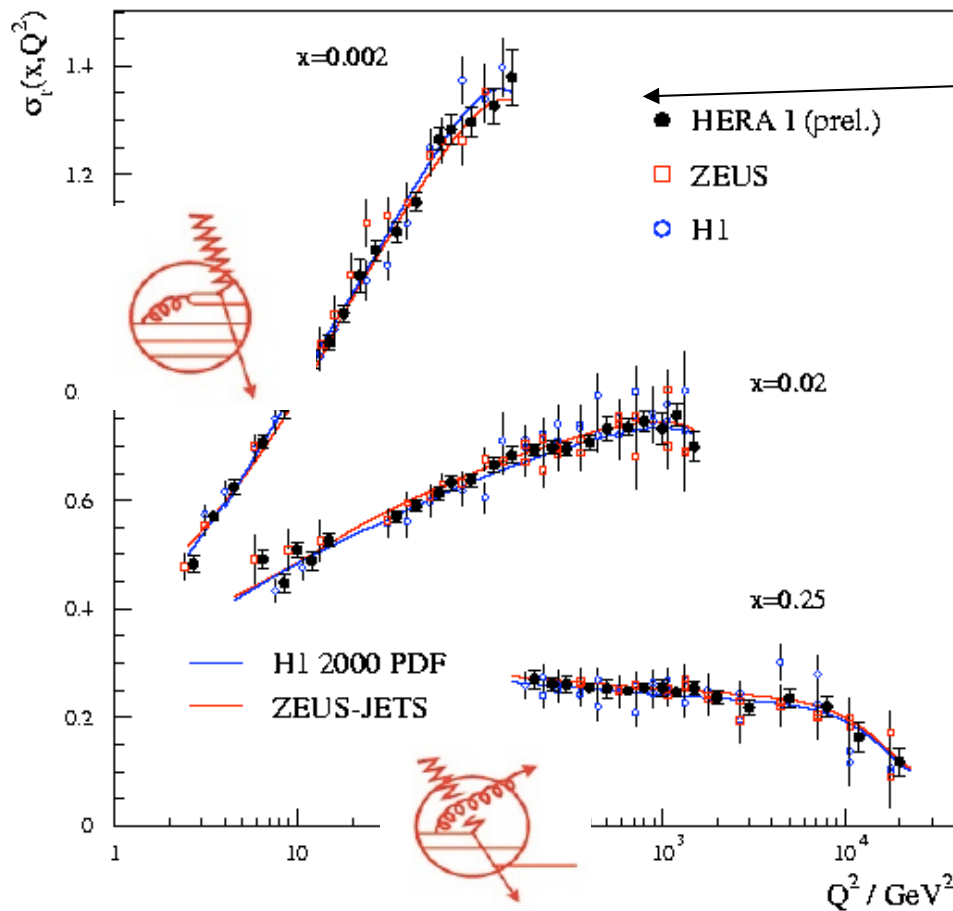
Method proposed at the
HERA-LHC Workshop

„theory-free“ Hessian fit,
which assumes a „true“
value of the cross
section.

$$\chi_{\text{exp}}^2 (M^{i,\text{true}}, \alpha_j) = \sum_i \frac{\left[M^{i,\text{true}} - \left(M^i + \sum_j \frac{\partial M^i}{\partial \alpha_j} \alpha_j \right) \right]^2}{\delta_i^2} + \sum_j \frac{\alpha_j^2}{\delta_{\alpha_j}^2}$$

Combined H1-ZEUS F_2

HERA 1 e^+p Neutral Current Scattering - H1 and ZEUS

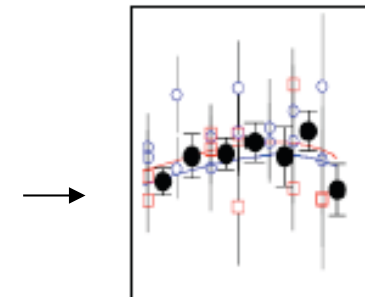


Precision ZEUS or H1
2-3%, <2% combined

DGLAP works, can
extract PDFs from fit

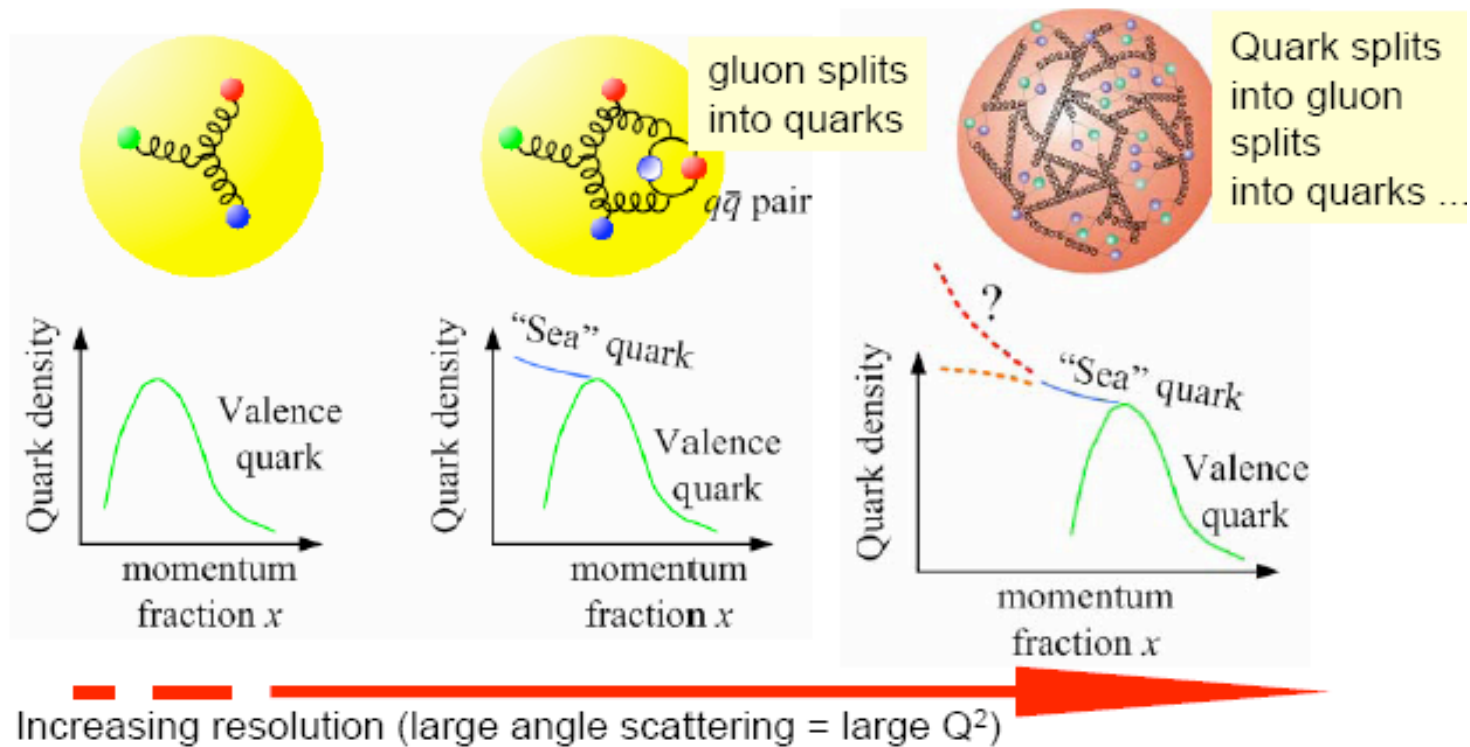
10% precision due to
statistics

Errors reduced in combination, each
experiment 'calibrates' the other



Parton densities

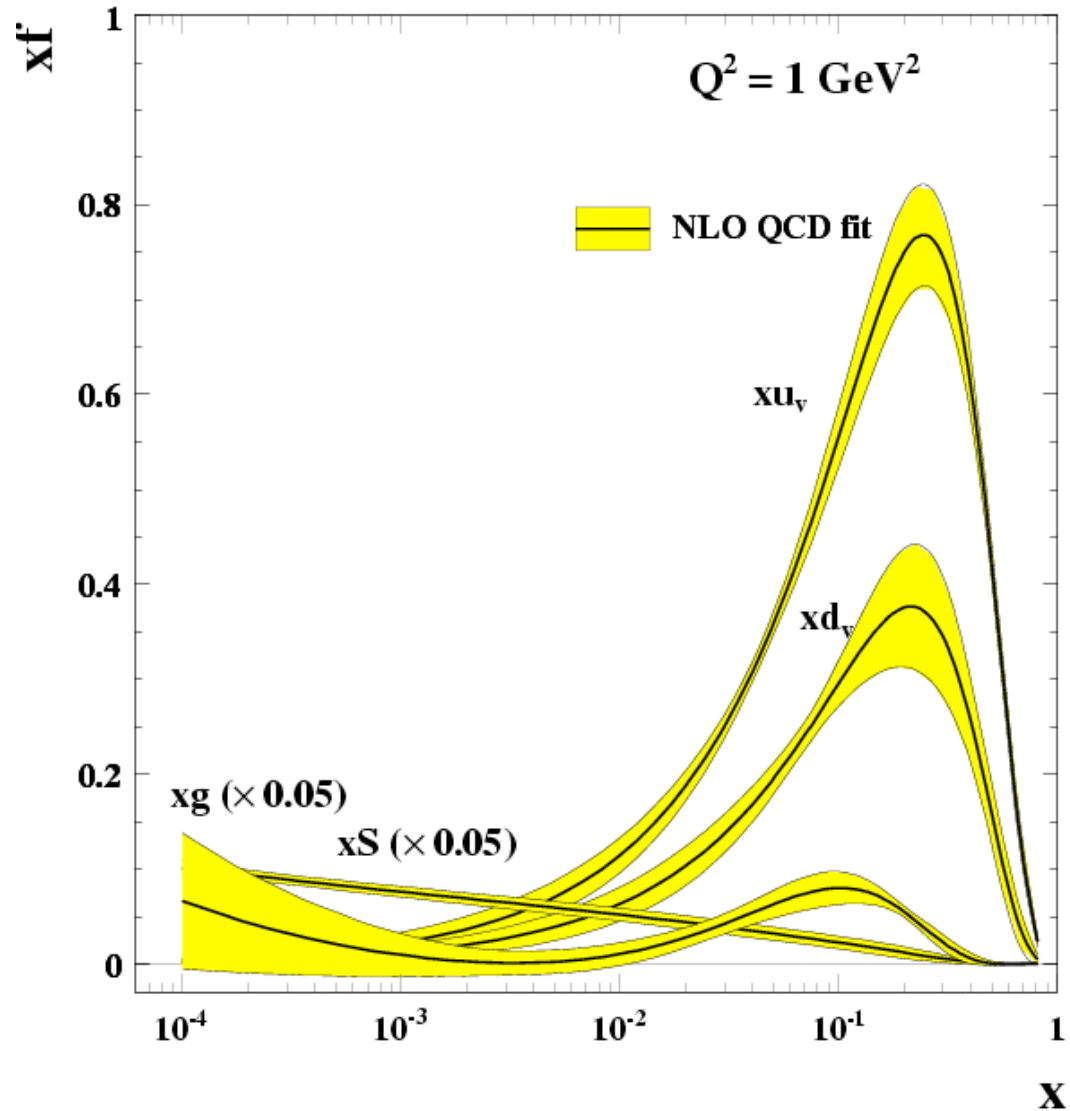
How does a parton density look like?



- Determine x_u, x_d, x_S, x_g from fits at a certain Q_0^2 and then evolve in Q^2 with the DGLAP evolution equations
- splitting functions calculated recently at NNLO

How does a parton density look like?

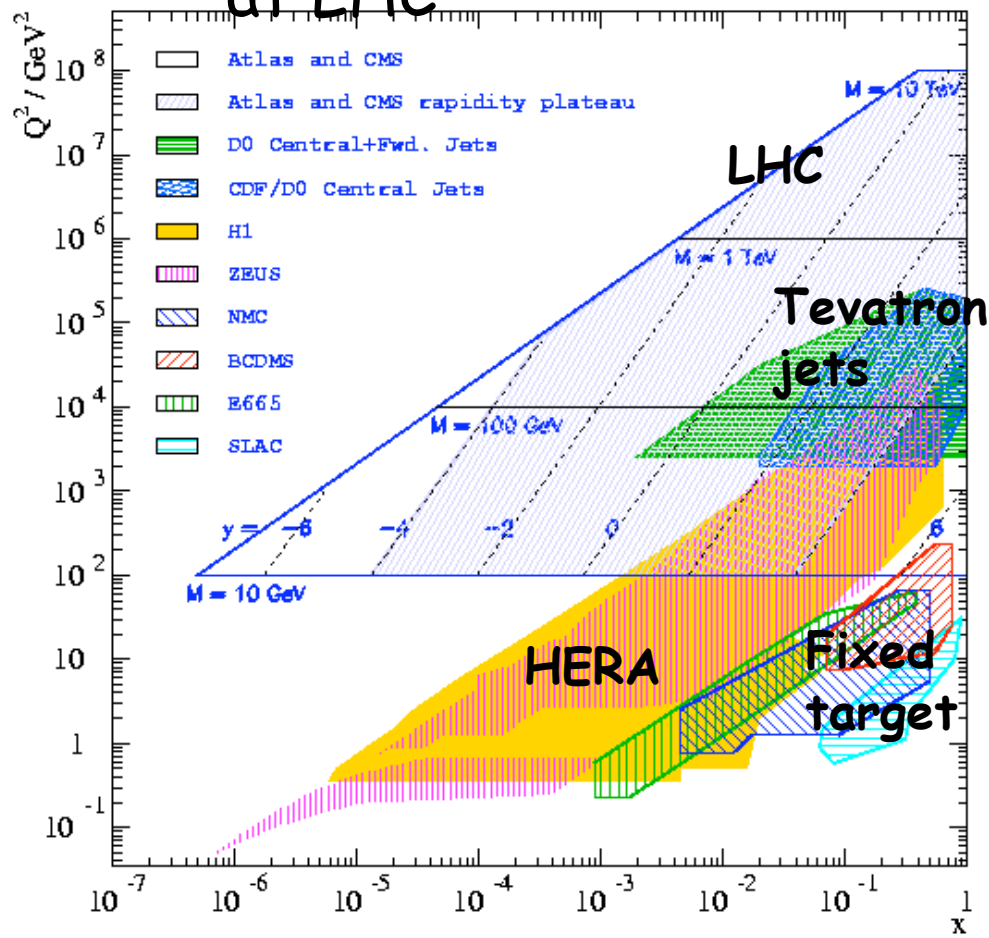
- u,d-valence, dominate at high x
- xS , sea, it is driven by the gluon, dominates at low x
- gluon, steep rise at low x
- evolution with Q^2 , example with a ZEUS QCD fit



Plot from C. Gwenlan and R. Yoshida

Data for parton densities

$$x_{1,2} = (M / \sqrt{s}) \exp(\pm y_{rap}) \sim 10^{-4} - 10^{-2} \text{ at LHC}$$



Data	PDFs
F_2	q, \bar{q} low x
$dF_2/d\ln Q_2$	g at low x
Fixed target	u, d, s
Tevatron jets	q, g high- x
Tevatron W	u/d large- x
Tevatron prompt γ	g
pN Drell-Yan	$\bar{u} - \bar{d}$

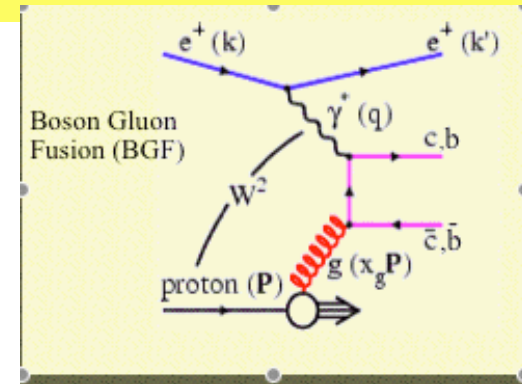
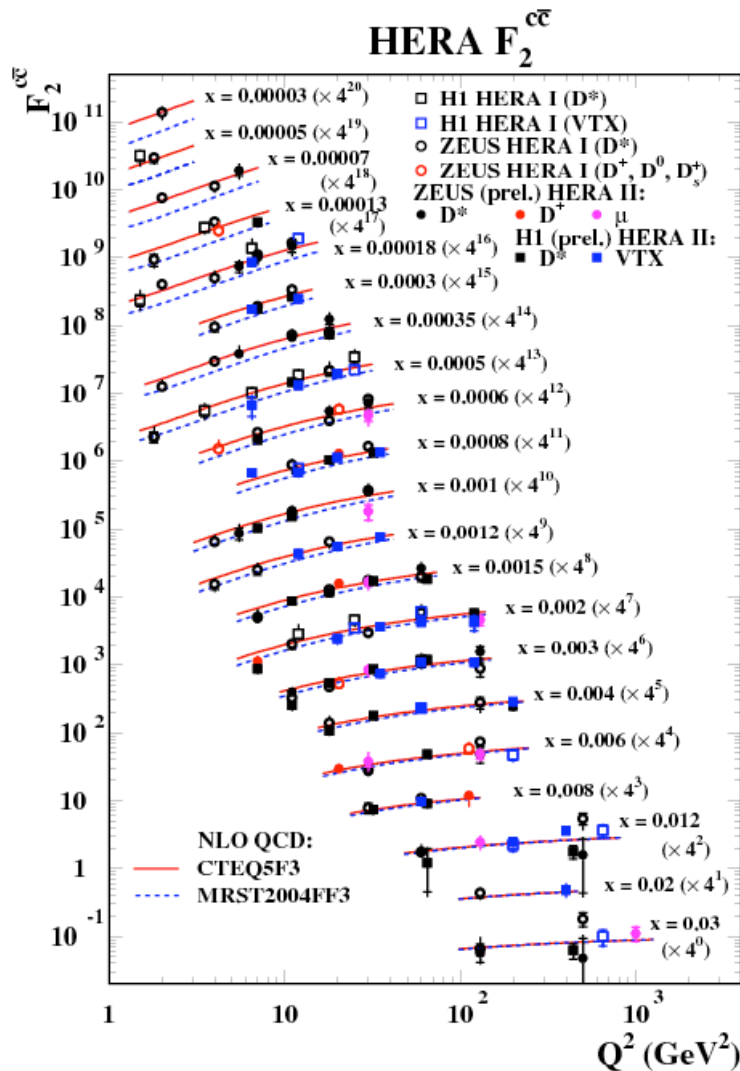
Example from MSTW2008

Data set	$\chi^2/N_{\text{pts.}}$
H1 MB 99 e^+p NC	9 / 8
H1 MB 97 e^+p NC	42 / 64
H1 low Q^2 96–97 e^+p NC	45 / 80
H1 high Q^2 98–99 e^-p NC	122 / 126
H1 high Q^2 99–00 e^+p NC	132 / 147
ZEUS SVX 95 e^+p NC	35 / 30
ZEUS 96–97 e^+p NC	86 / 144
ZEUS 98–99 e^-p NC	54 / 92
ZEUS 99–00 e^+p NC	62 / 90
H1 99–00 e^+p CC	29 / 28
ZEUS 99–00 e^+p CC	38 / 30
H1/ZEUS ep F_2^{charm}	108 / 83
H1 99–00 e^+p incl. jets	19 / 24
ZEUS 96–97 e^+p incl. jets	29 / 30
ZEUS 98–00 $e^\pm p$ incl. jets	16 / 30
DØ I $p\bar{p}$ incl. jets	68 / 90
CDF II $p\bar{p}$ incl. jets	73 / 76
CDF II $W \rightarrow l\nu$ asym.	29 / 22
DØ II $W \rightarrow l\nu$ asym.	23 / 10
DØ II Z rap.	19 / 28
CDF II Z rap.	35 / 29

Data set	$\chi^2/N_{\text{pts.}}$
BCDMS μp F_2	182 / 163
BCDMS μd F_2	187 / 151
NMC μp F_2	121 / 123
NMC μd F_2	103 / 123
NMC $\mu n/\mu p$	130 / 148
E665 μp F_2	57 / 53
E665 μd F_2	53 / 53
SLAC ep F_2	30 / 37
SLAC ed F_2	40 / 38
NMC/BCDMS/SLAC F_L	38 / 31
E866/NuSea pp DY	227 / 184
E866/NuSea pd/pp DY	15 / 15
NuTeV νN F_2	50 / 53
CHORUS νN F_2	26 / 42
NuTeV νN $x F_3$	40 / 45
CHORUS νN $x F_3$	31 / 33
CCFR $\nu N \rightarrow \mu\mu X$	65 / 86
NuTeV $\nu N \rightarrow \mu\mu X$	39 / 40
All data sets	2497 / 2723

- Red = Update to last MRST fit.

Charm, beauty



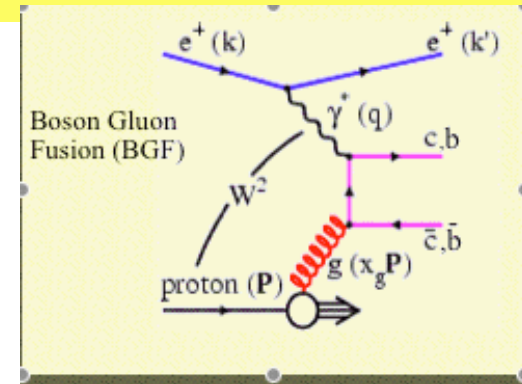
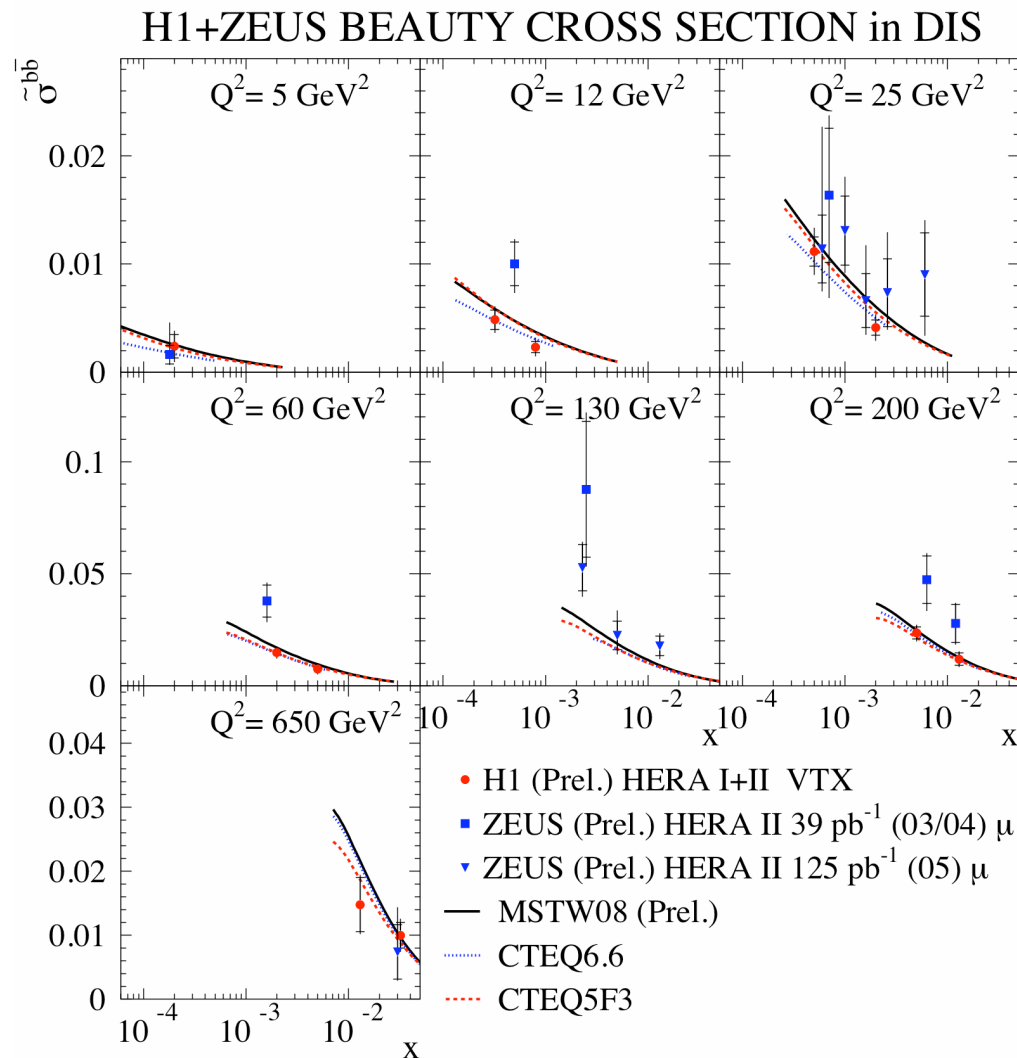
• For $Q^2 \sim m_c^2$ the charm does not act as a parton, BGF process, **massive** scheme (FFNS)

For $Q^2 \gg m_c^2$ the charm behaves as a **massless** parton (ZM-VFNS)

Variable number scheme in between (GM-VFNS)

Different schemes, quite different predictions, data increasing precision

Charm, beauty



• For $Q^2 \sim m_c^2$ the charm does not act as a parton, BGF process, **massive** scheme (FFNS)

For $Q^2 \gg m_c^2$ the charm behaves has a **massless** parton (ZM-VFNS)

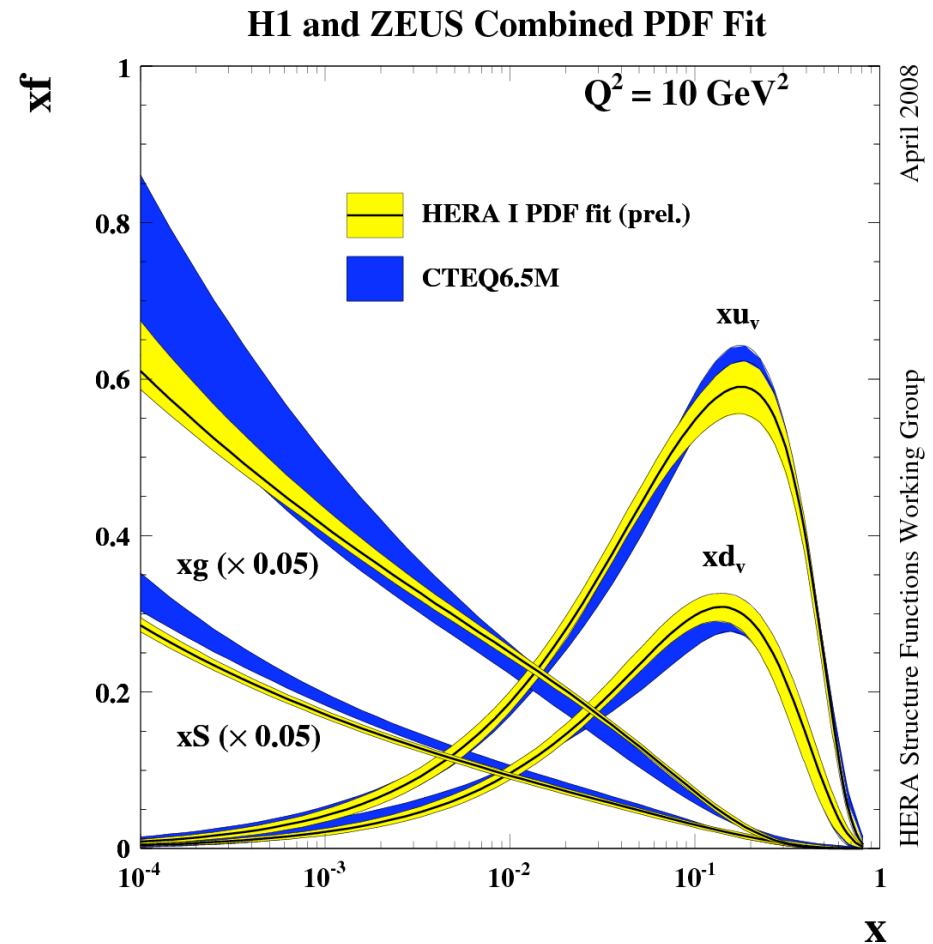
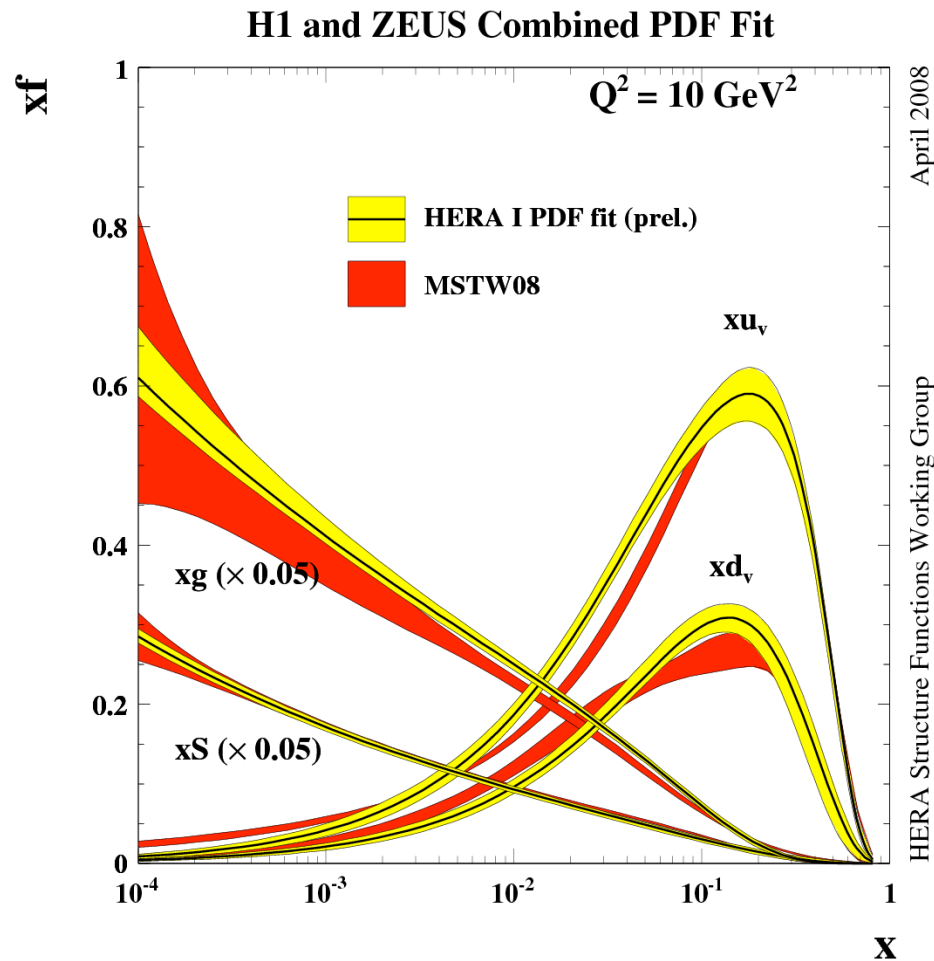
Variable number scheme in between (GM-VFNS)

Different schemes, quite different predictions, data increasing precision

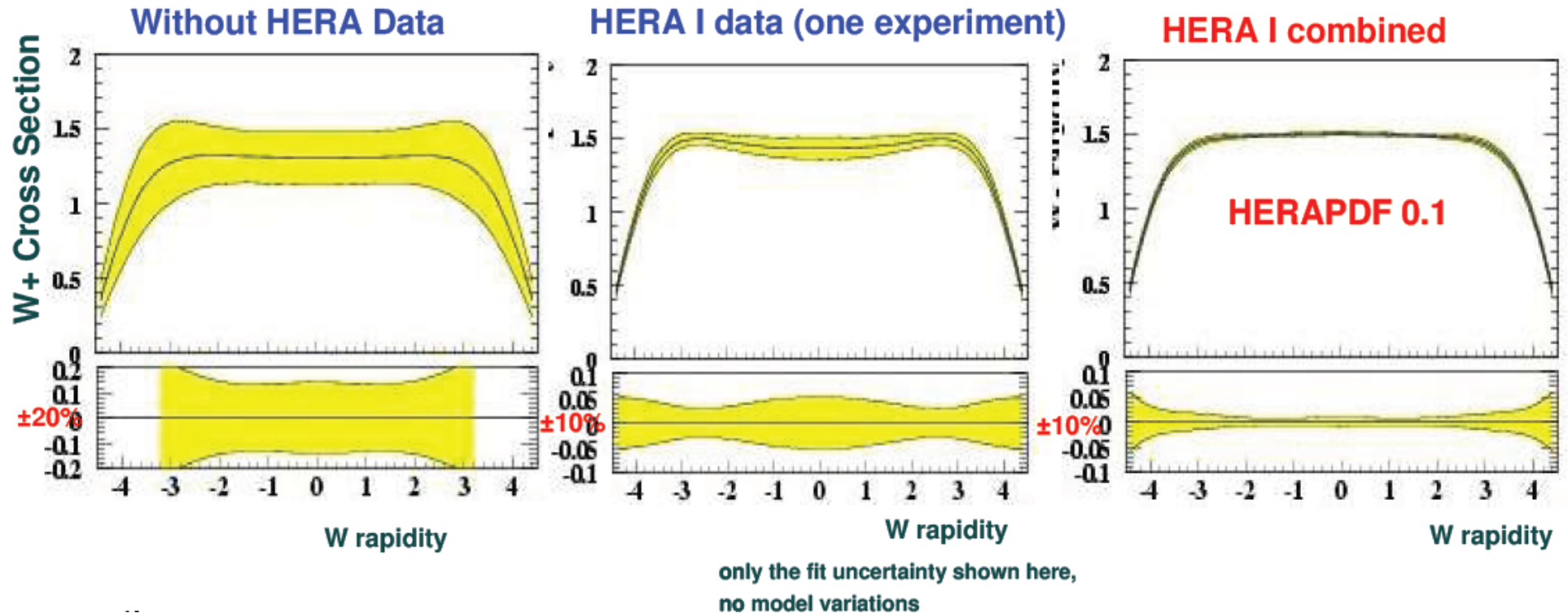
Parton densities from combined HERA data

HERA I PDF Fit using
HERA data only

- no heavy target corrections
- control of systematic errors



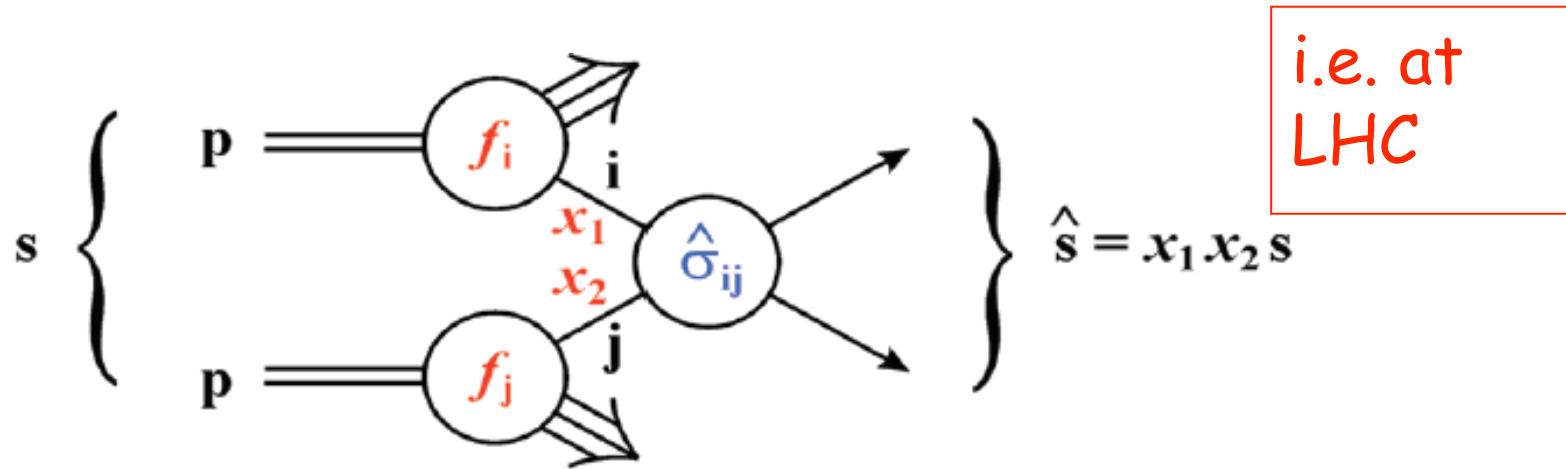
Parton densities from combined data



A test on a standard candle process at LHC

HERA PDFs 0.1 available in LHAPDF

Factorization property in hard scattering

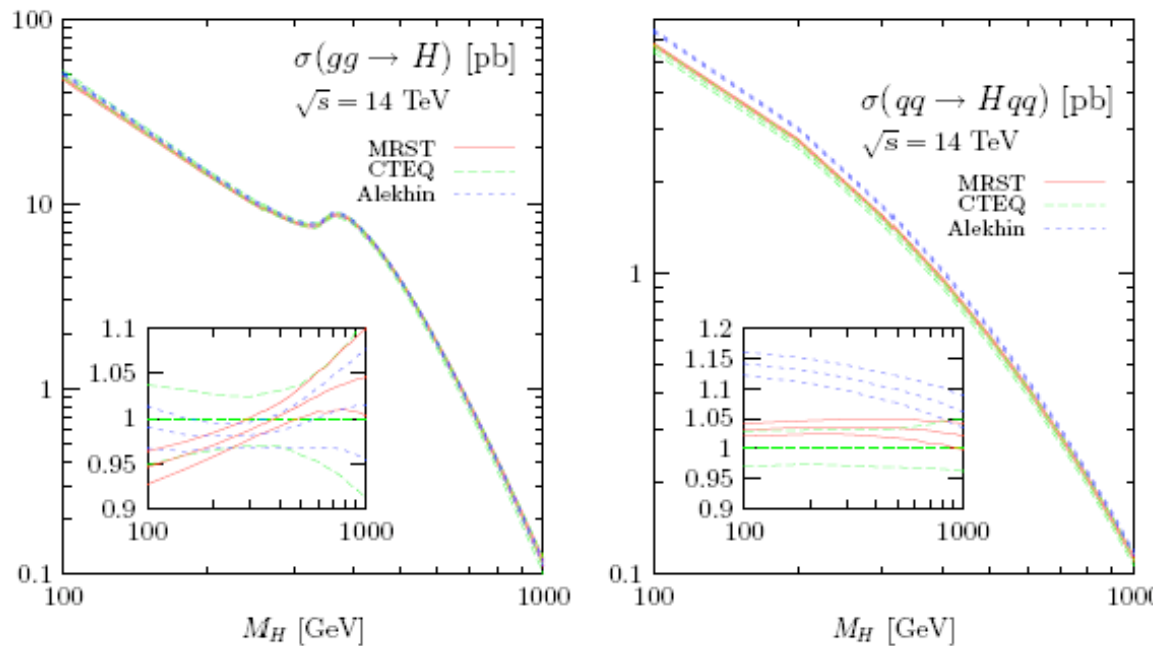


$$\sigma = \sum_{i,j} \int dx_1 dx_2 \underbrace{f_i(x_1, Q^2) f_j(x_2, Q^2)}_{\text{red}} \underbrace{\hat{\sigma}_{ij}(x_1 x_2 s, \alpha_S(Q^2))}_{\text{blue}}$$

Non-perturbative, parton densities, universal, from fit to exps. data

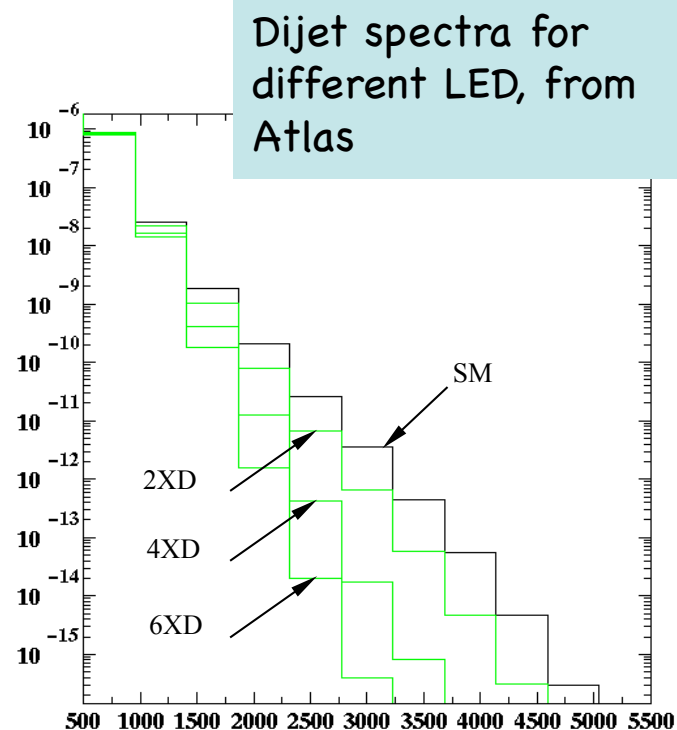
Perturbative process, calculable in pQCD

PDFs in discoveries at LHC

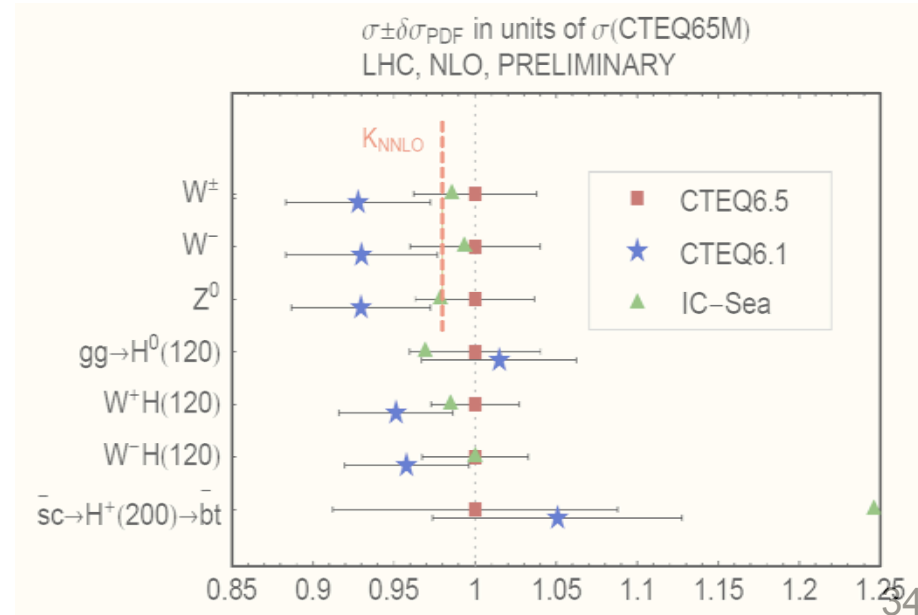
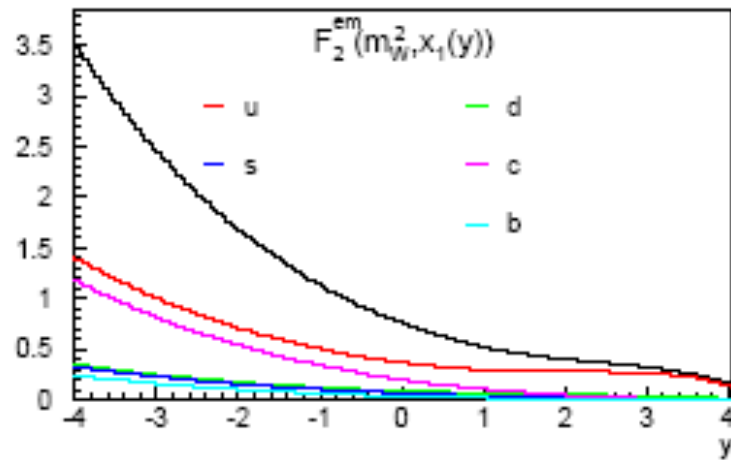
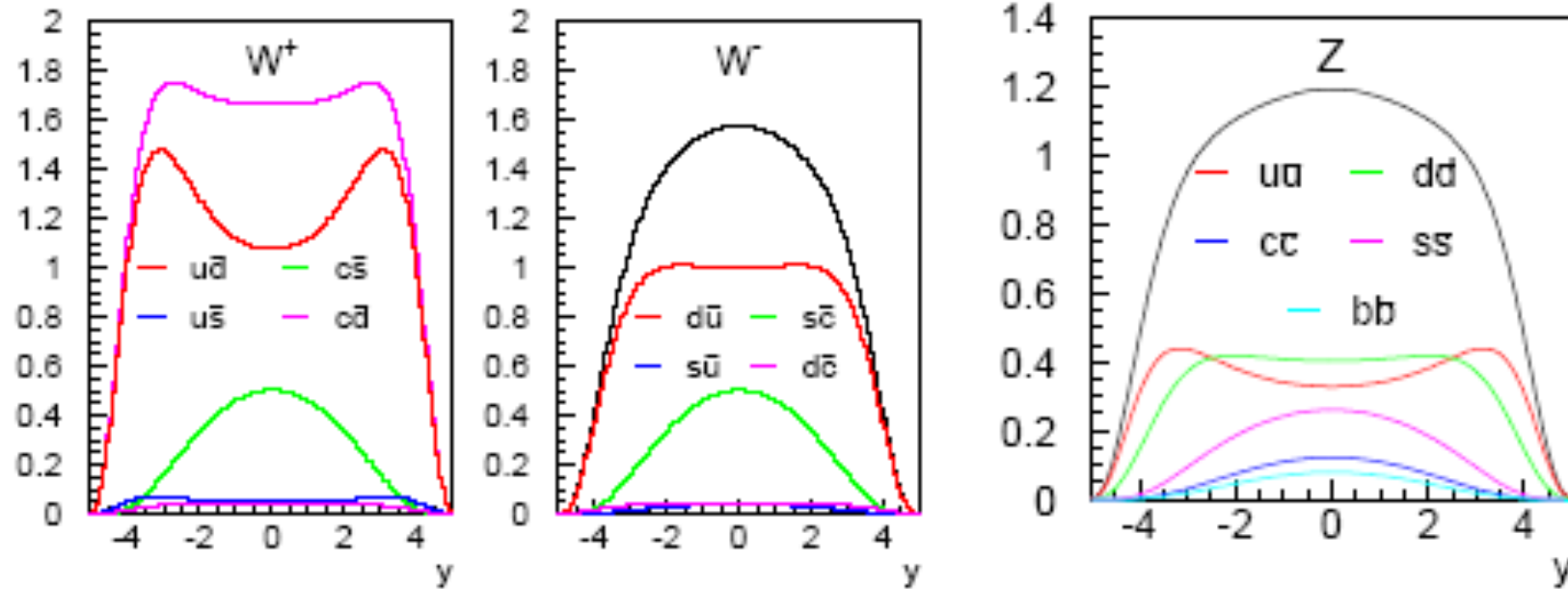


Some other, like LED, depend on precision understanding of PDFs

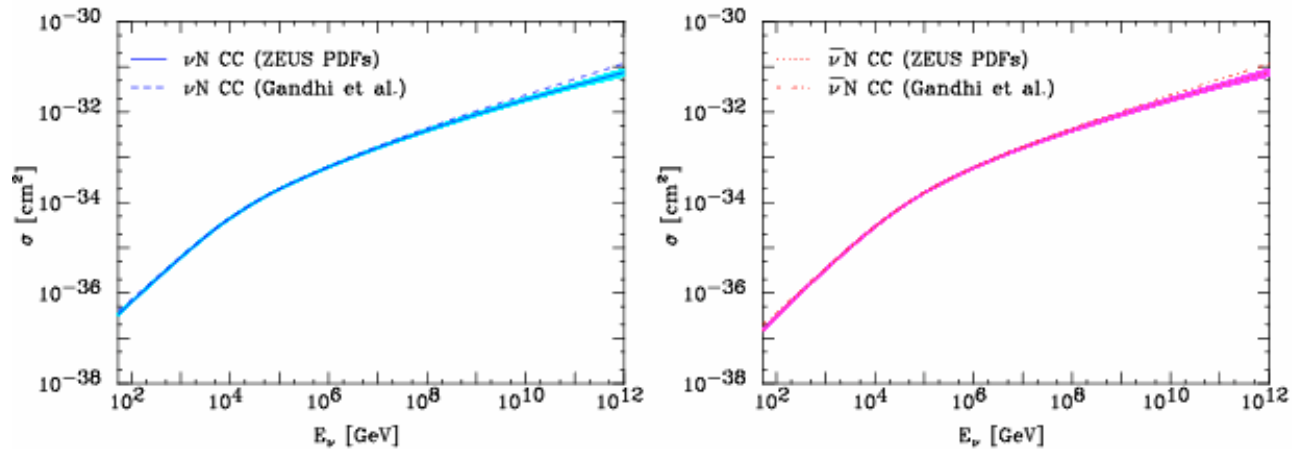
Some LHC discoveries, i.e. Higgs, not really affected by PDFs



c,b contribution at LHC



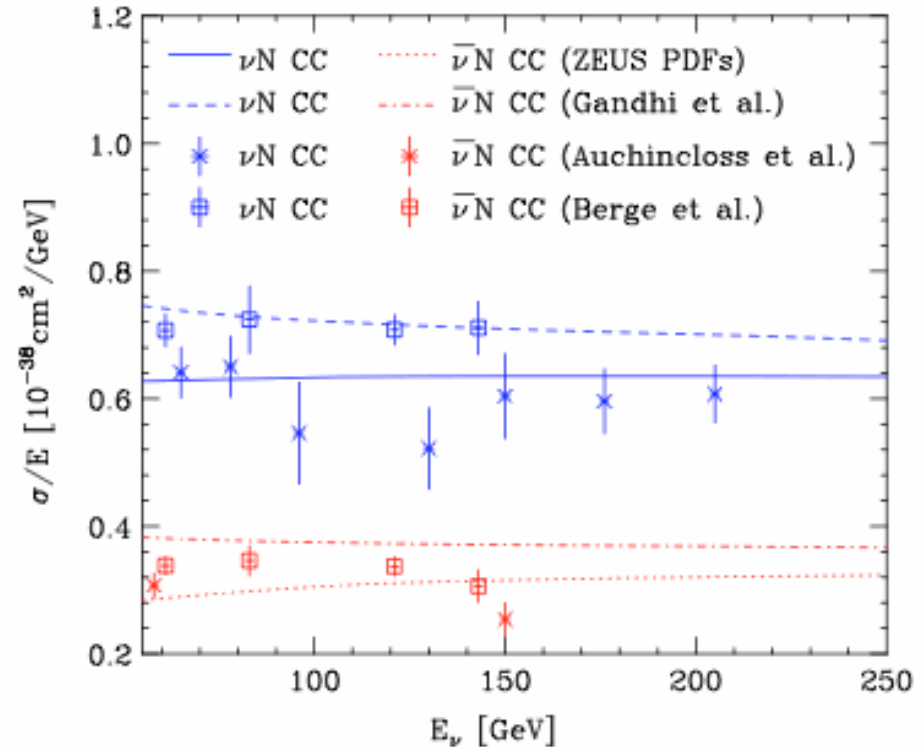
PDFs in astroparticle physics



i.e. $\sigma(\nu N) = [Y_+ F_2^\nu(x, Q^2) - y^2 F_L^\nu(x, Q^2) + Y_- x F_3^\nu(x, Q^2)]$

M. Cooper-Sarkar, S.
Sarkar arViv:0710.5303

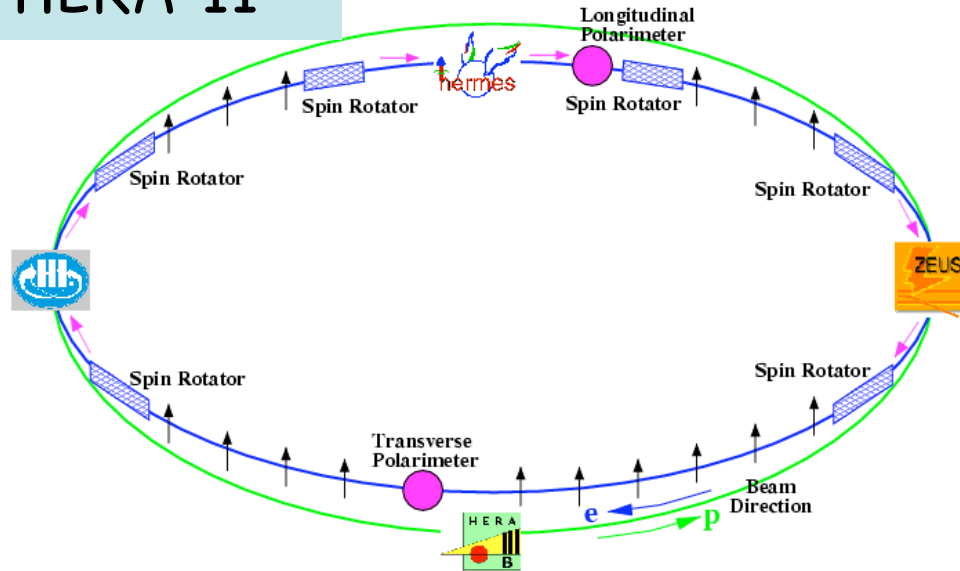
Update of the neutrino cross-sections as used in astroparticle physics, using all tools typical of a HERA PDF analysis, extending it to $Q^2=10^{12} \text{ GeV}^2$ and $x=10^{-12}$.



Structure functions and polarization

Polarized CC

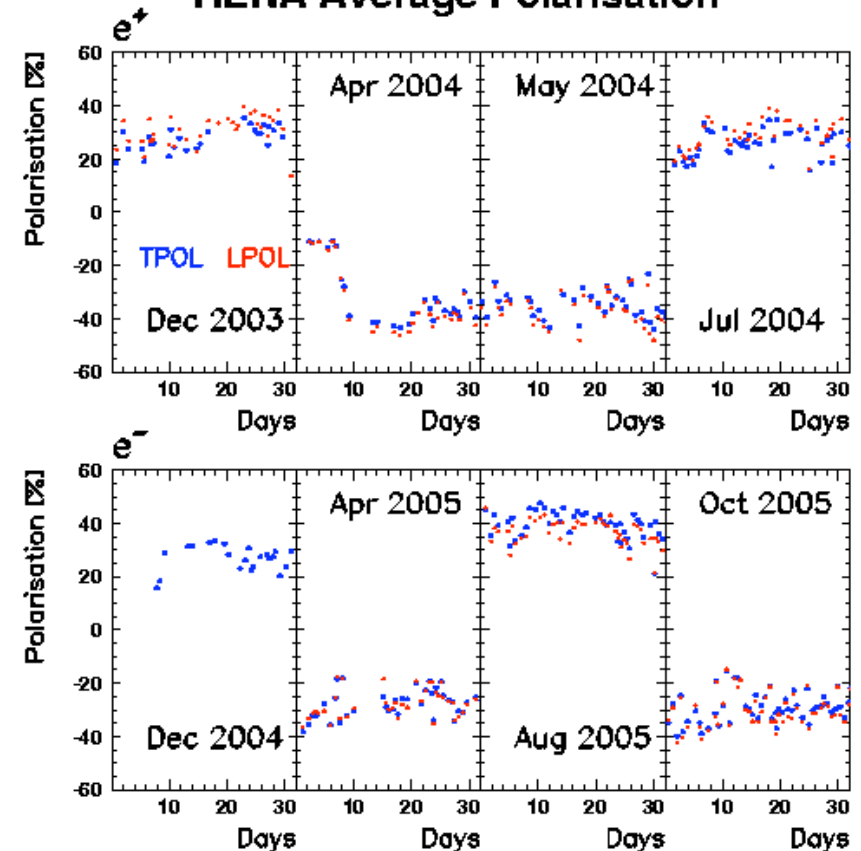
HERA II



Lepton naturally transversely polarized (Sokolov-Ternov effect) with a build-up time of 30 minutes. Spin rotators to provide longitudinally polarized beams at the experiments.

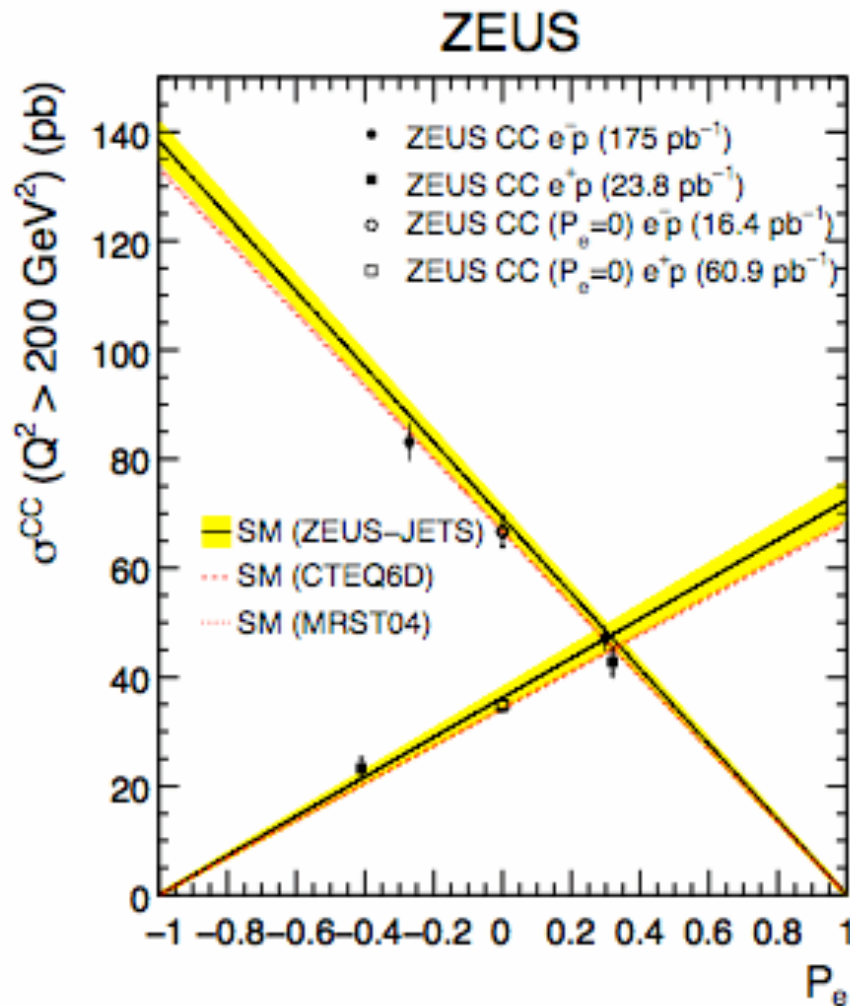
Lepton polarization 30–40%, changed every 2–3 months, equal lumi for e⁺, e⁻, LH and RH. Polarization measured by three independent devices

HERA Average Polarisation



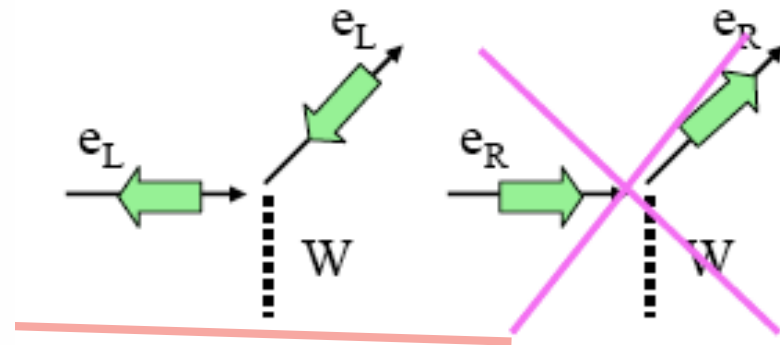
$$P = (N_R - N_L) / (N_R + N_L)$$

Polarized CC

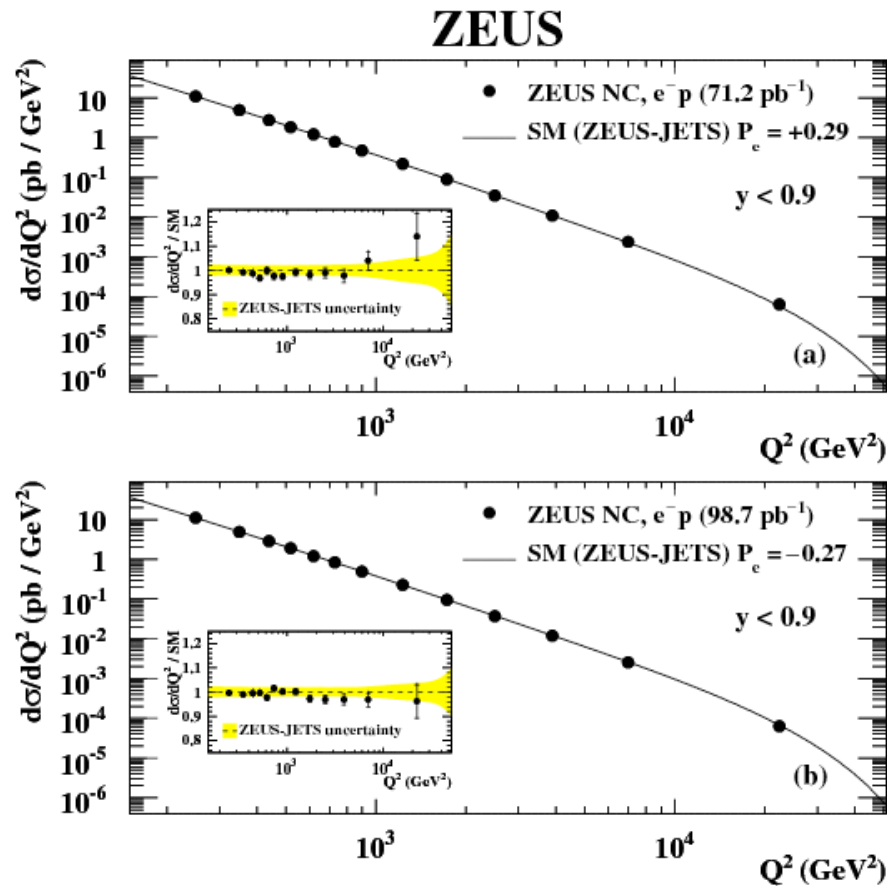


$$\sigma_{\text{polCC}}^{e\pm p}(Q^2, X) = \frac{1 \pm P_e}{2} \cdot \sigma_{\text{LHCC}}^{e\pm p}(Q^2, X)$$

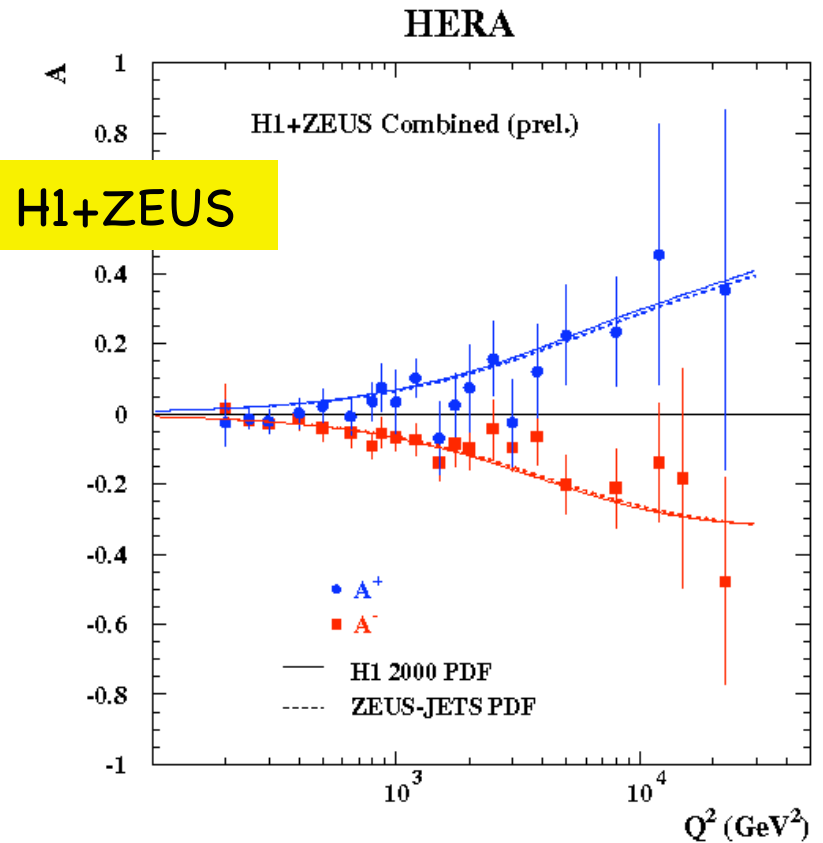
Another textbook plot,
absence of right-handed
charged current



Polarized NC at high Q^2



$$A^\pm = \frac{2}{P_R - P_L} \cdot \frac{\sigma^\pm(P_R) - \sigma^\pm(P_L)}{\sigma^\pm(P_R) + \sigma^\pm(P_L)} \simeq \mp k a_e \frac{F_2^{\gamma Z}}{F_2}$$



In NC the effect of P is small, but one can measure the asymmetry: parity-violating effect observed in NC at high Q^2 for the first time

Polarized QCD fits

$$\sigma_r(e^\pm p) = (Y_+ F_2^0 \mp Y_- x F_3^0) \mp P(Y_- F_2^P \mp Y_+ x F_3^P)$$

$$F_2^{0,P} = \sum_i A_i^{0,P}(Q^2) [xq_i(x, Q^2) + x\bar{q}(x, Q^2)]$$

$$xF_3^{0,P} = \sum_i B_i^{0,P}(Q^2) [xq_i(x, Q^2) - x\bar{q}(x, Q^2)]$$

$$A^0(Q^2) = -e_i^2 - 2e_i v_i v_e P_Z + (v_e^2 + a_e^2)(v_i^2 + a_i^2) P_Z^2$$

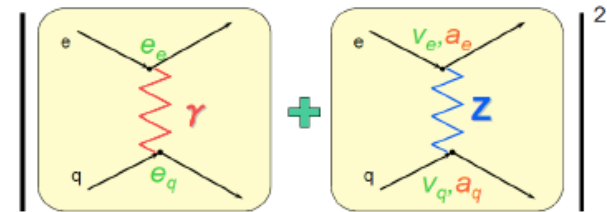
$$B_i^0(Q^2) = -2e_i a_i a_e P_Z + 4a_i a_e v_i v_e P_Z^2$$

$$A_i^P(Q^2) = -2e_i v_i a_e P_Z - 2v_e a_e (v_i^2 + a_i^2) P_Z^2$$

$$B_i^P(Q^2) = -2e_i a_i v_e P_Z - 2v_i a_i (v_e^2 + a_e^2) P_Z^2$$

Neutral current cross-section

Polarized structure functions



Unpolarized xF_3 determines the axial couplings

Polarized F_2 determines the vector couplings

Parton densities and Z-couplings fitted at the same time

Polarized QCD fits

$$\sigma_r(e^\pm p) = (Y_+ F_2^0 \mp Y_- x F_3^0) \mp P(Y_- F_2^P \mp Y_+ x F_3^P)$$

$$F_2^{0,P} = \sum_i A_i^{0,P}(Q^2) [xq_i(x, Q^2) + x\bar{q}(x, Q^2)]$$

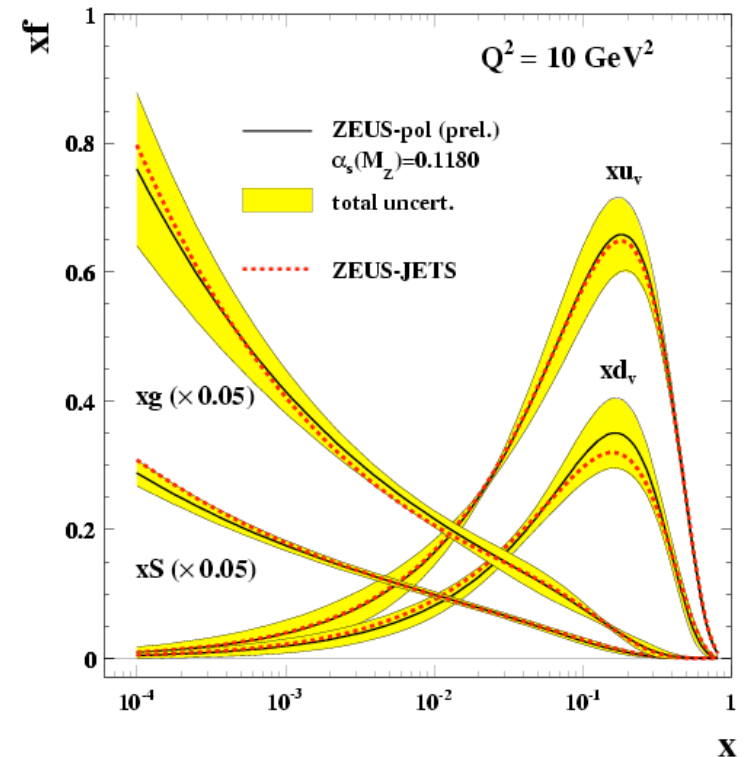
$$xF_3^{0,P} = \sum_i B_i^{0,P}(Q^2) [xq_i(x, Q^2) - x\bar{q}(x, Q^2)]$$

$$A^0(Q^2) = -e_i^2 - 2e_i v_i v_e P_Z + (v_e^2 + a_e^2)(v_i^2 + a_i^2) P_Z^2$$

$$B_i^0(Q^2) = -2e_i a_i a_e P_Z + 4a_i a_e v_i v_e P_Z^2$$

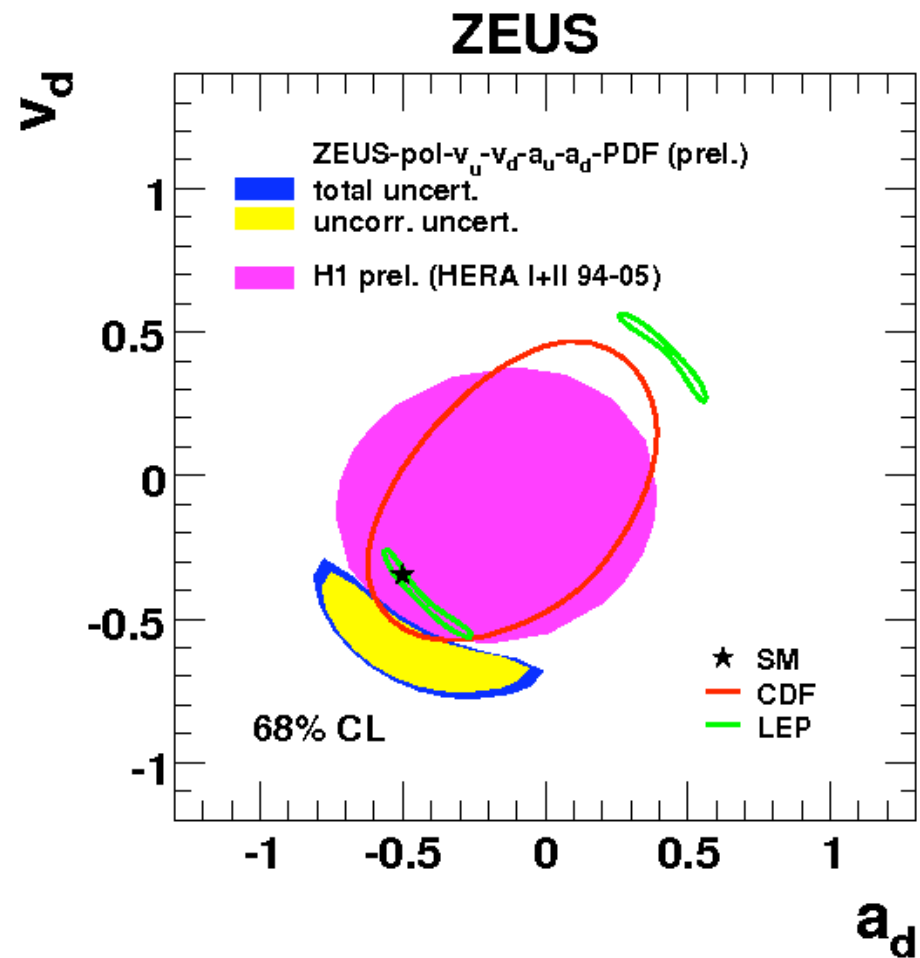
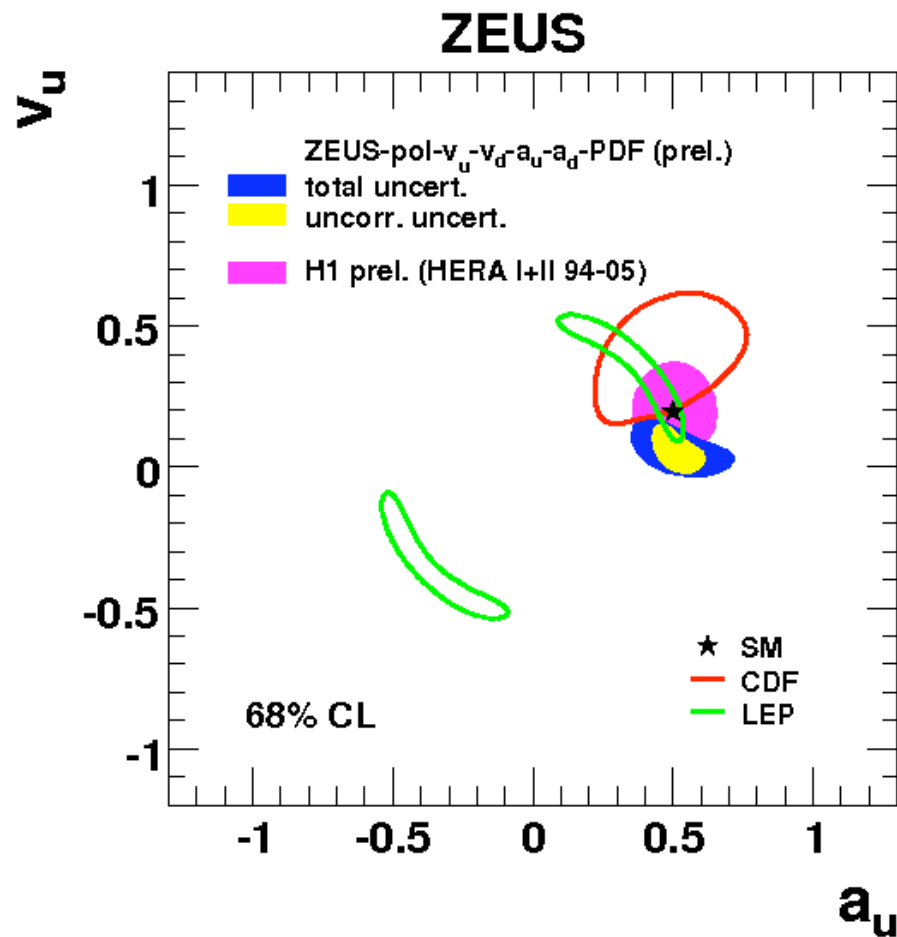
$$A_i^P(Q^2) = -2e_i v_i a_e P_Z - 2v_e a_e (v_i^2 + a_i^2) P_Z^2$$

$$B_i^P(Q^2) = -2e_i a_i v_e P_Z - 2v_i a_i (v_e^2 + a_e^2) P_Z^2$$



Parton densities and Z-couplings fitted at the same time

Polarized QCD fits



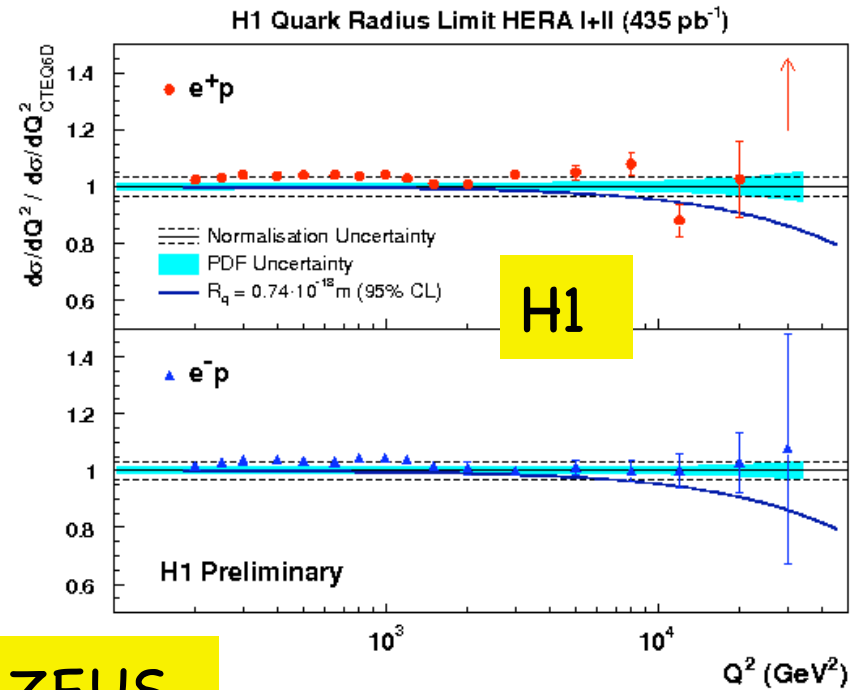
Vector and axial couplings for u- and d- quarks determined with competitive precision, in agreement with SM

Quark radius

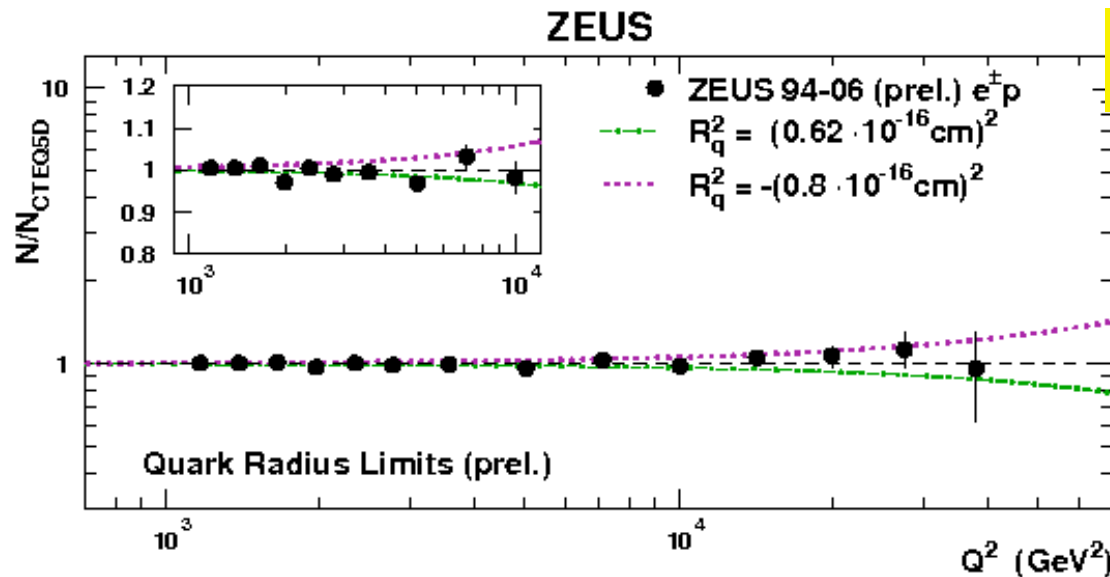
Can be determined as a form factor,
assume electron pointlike:

$$\frac{d\sigma}{dQ^2} = \frac{d\sigma^{SM}}{dQ^2} \cdot [1 - (R_q^2/6)Q^2]^2 \cdot [1 - (R_e^2/6)Q^2]^2$$

$$R_q < 0.74 \times 10^{-16} \text{ cm}$$



ZEUS

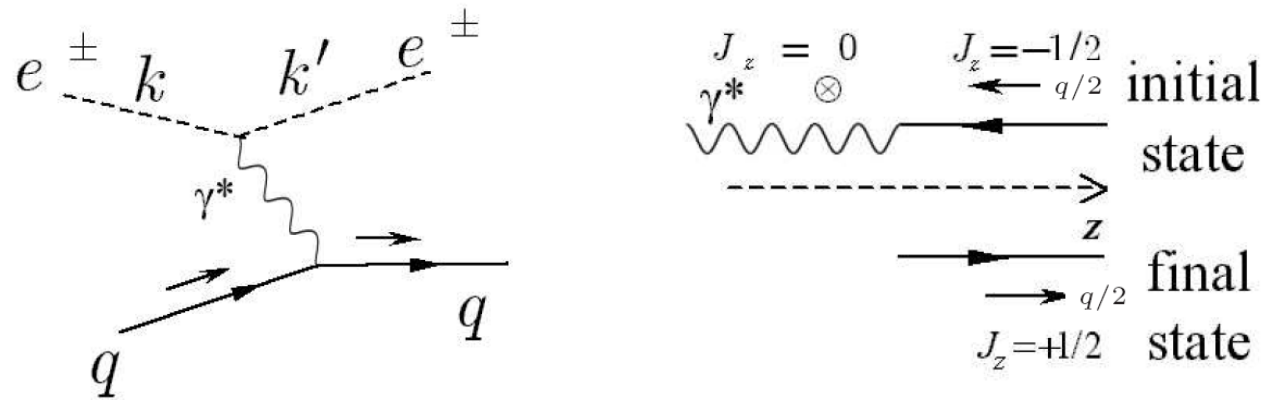


$$R_q < 0.62 \times 10^{-16} \text{ cm}$$

Most stringent limit today

Measurement of F_L

F_L in QCD



In QPM:

$$F_L \sim \sigma_L \gamma^P = 0$$

$$F_L = F_2 - 2xF_1 = 0$$

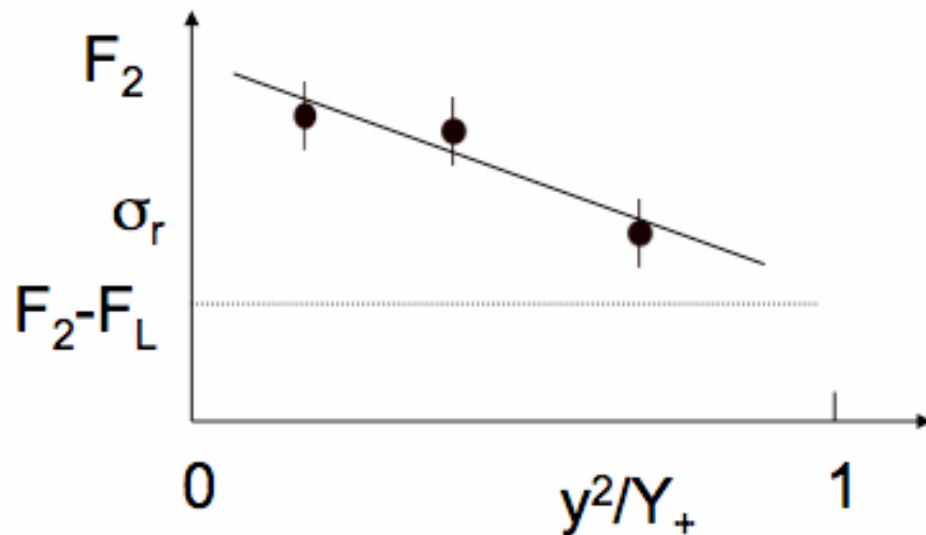
Callan-Gross relation

In QCD: $F_L \neq 0$

$$F_L = \frac{\alpha_s}{4\pi} x^2 \int_x^1 \frac{dz}{z^3} \left[\frac{16}{3} F_2 + 8 \sum e_q^2 (1 - x/z) z g \right]$$

Depends
directly on the
gluon

The method to measure F_L

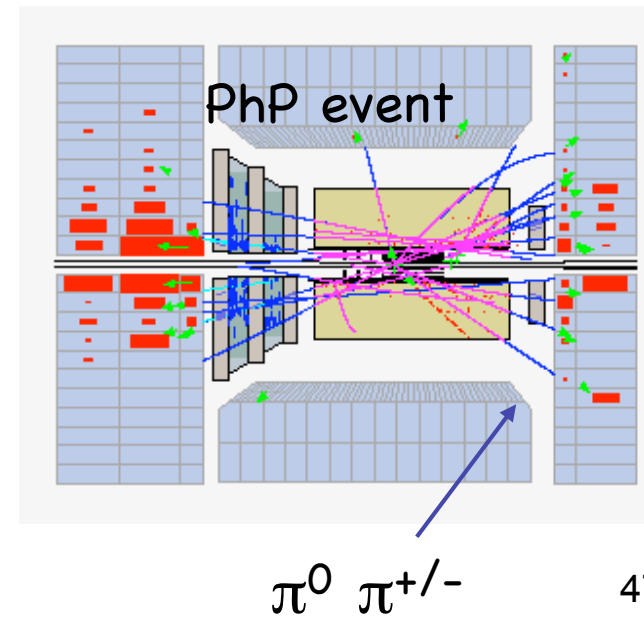
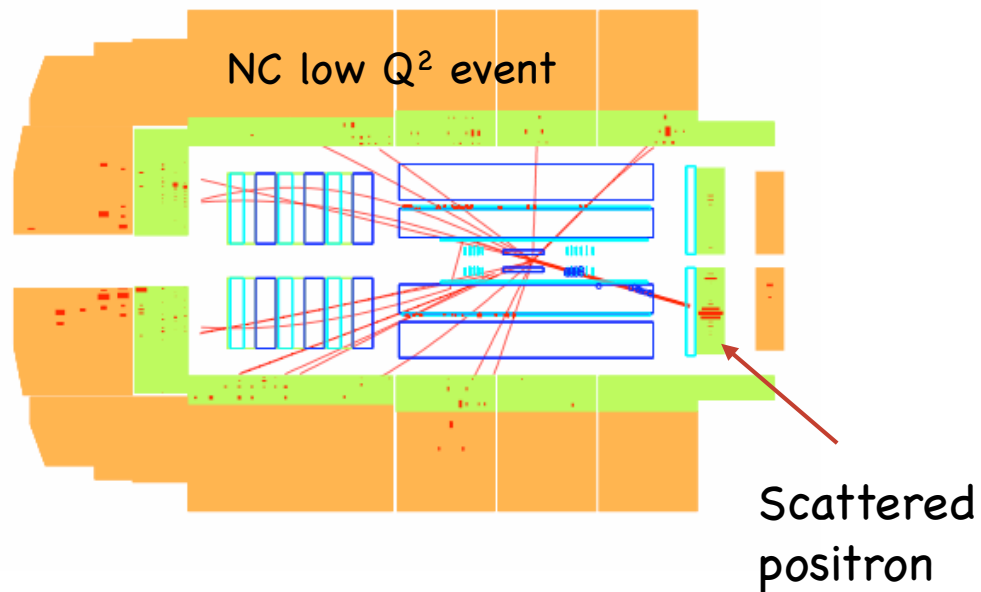
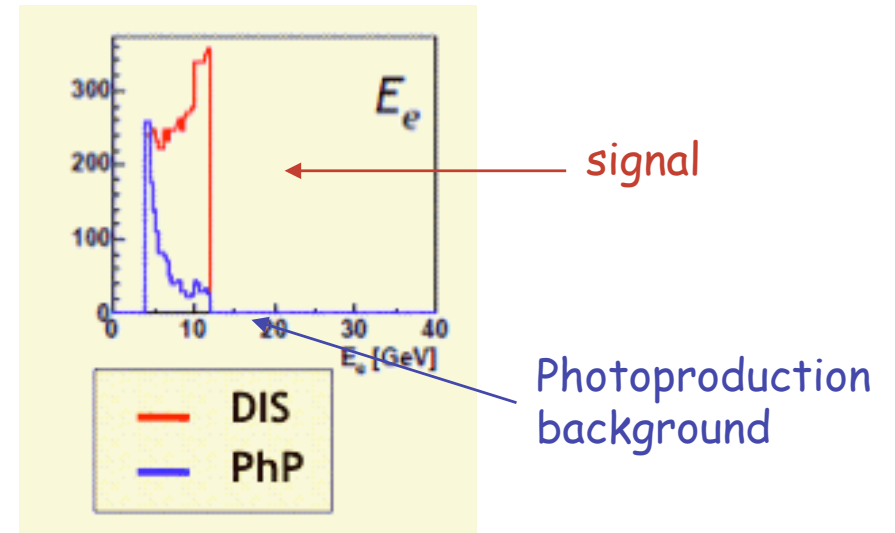
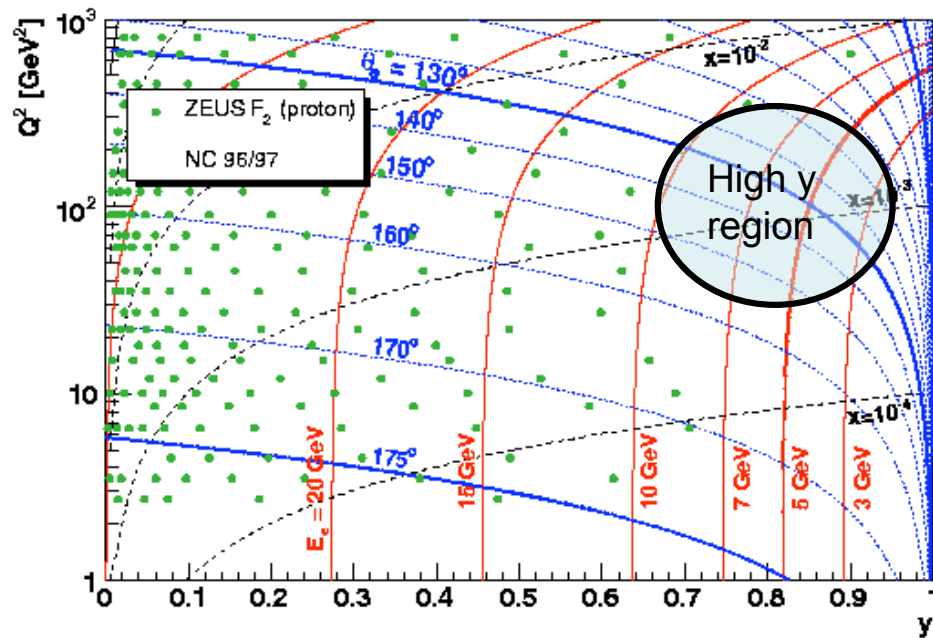


$$\sigma_r = \frac{xQ^4}{2\pi\alpha^2(1+(1-y)^2)} \frac{d^2\sigma(e^\mp p)}{dx dQ^2}$$

$$\approx \left[F_2 - \frac{y^2}{(1+(1-y)^2)} F_L \right]$$

- o Measure the same reduced xsec at the same (x, Q^2) and different y , that is different s ($y=Q^2/xs$).
- o This was realized in March-June 2007 changing the proton beam energy to $E_p=460$ GeV and $E_p=570$ GeV (14 pb⁻¹ at 460 GeV, 7 pb⁻¹ at 575 GeV)
- o The LER measurement is at very high y , low scattered positron energy (trigger, detection, efficiency, background)

Challenges of the measurement

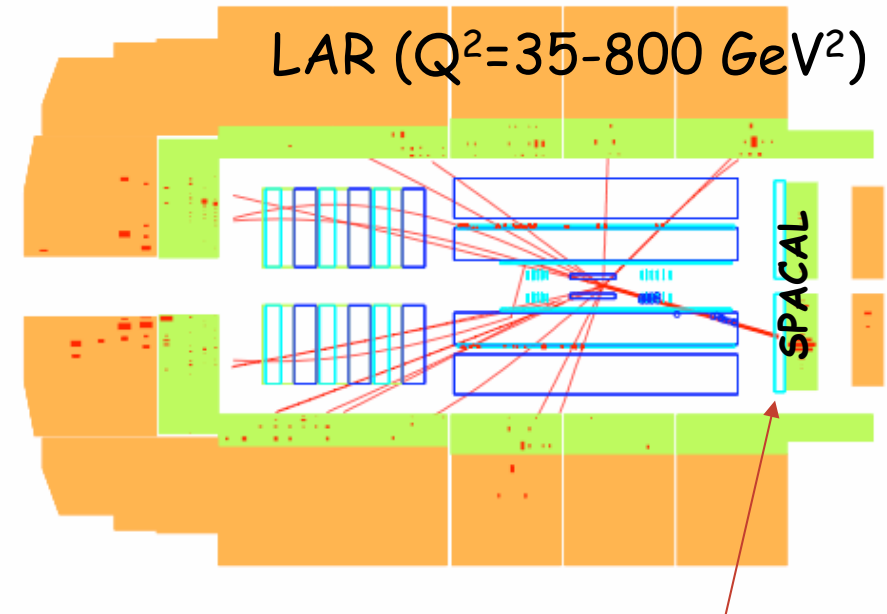
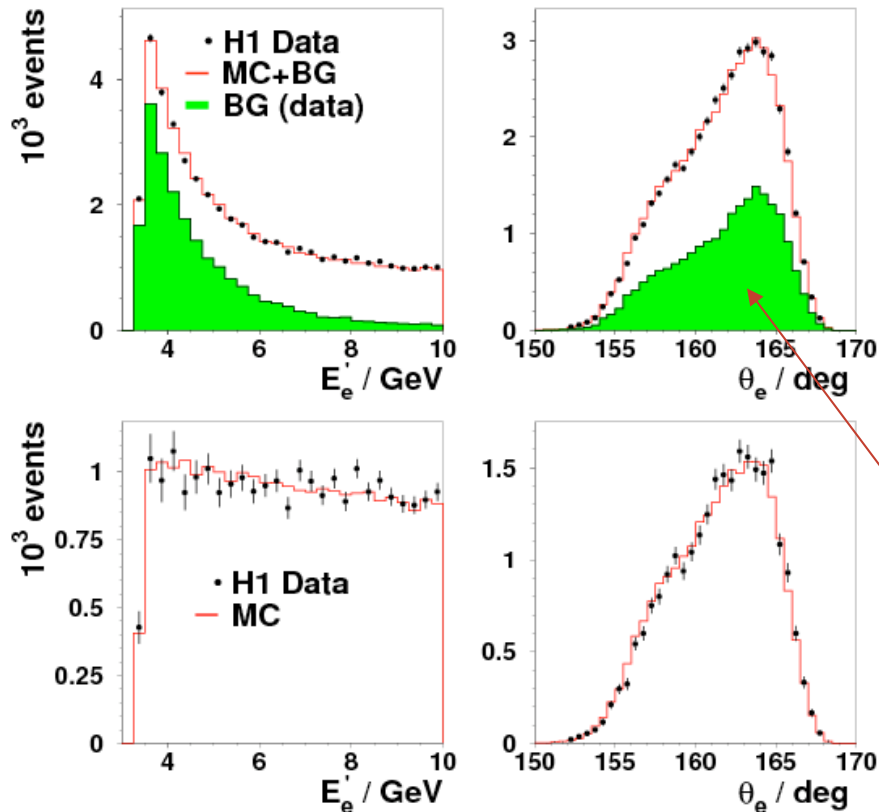


Challenges in H1

$$E_e > 3 \text{ GeV}, y < 0.9$$

$$12 < Q^2 < 800 \text{ GeV}^2$$

Photoproduction background controlled with charge asymmetry



($Q^2=12-90 \text{ GeV}^2$)
Published in PLB

Background determined from „wrong“ charge

Challenges in ZEUS

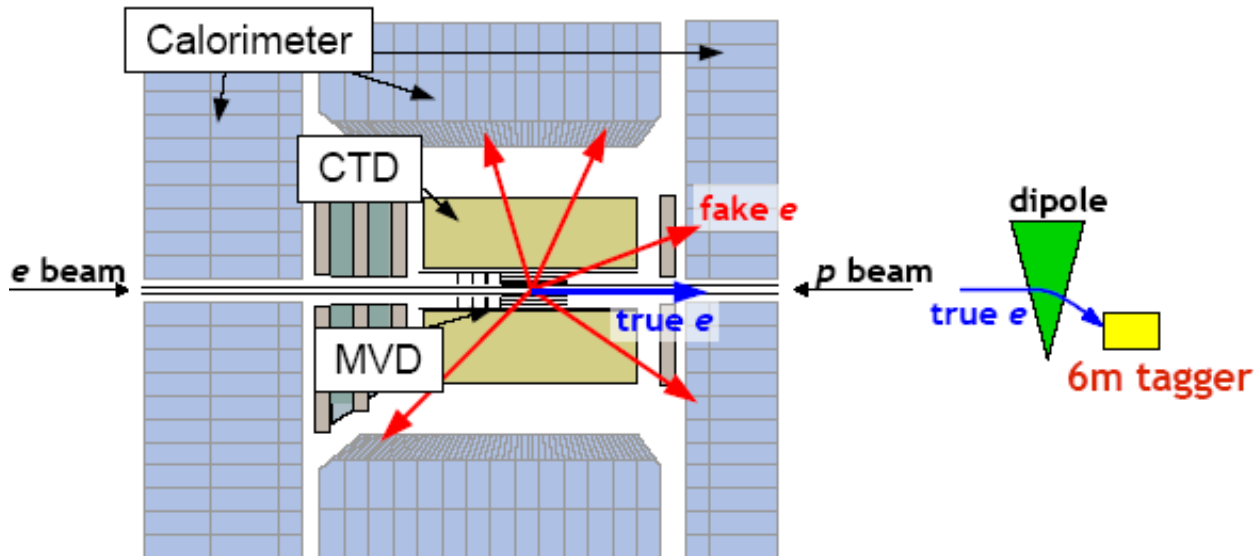
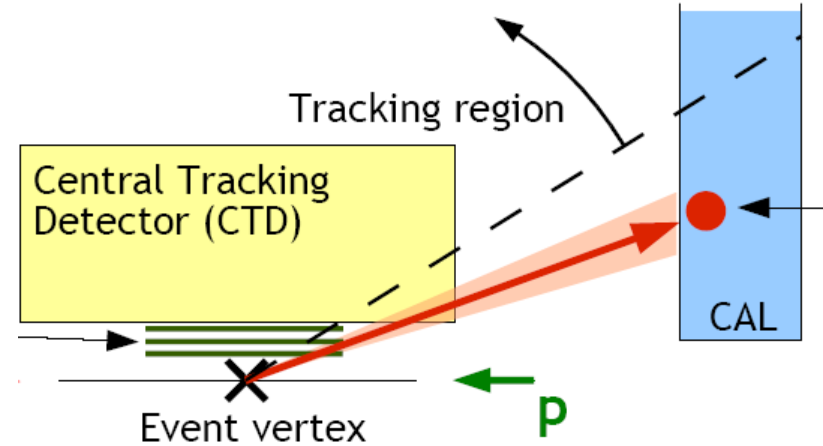
$$E_e > 6 \text{ GeV}, y < 0.76$$

$$24 < Q^2 < 110 \text{ GeV}^2$$

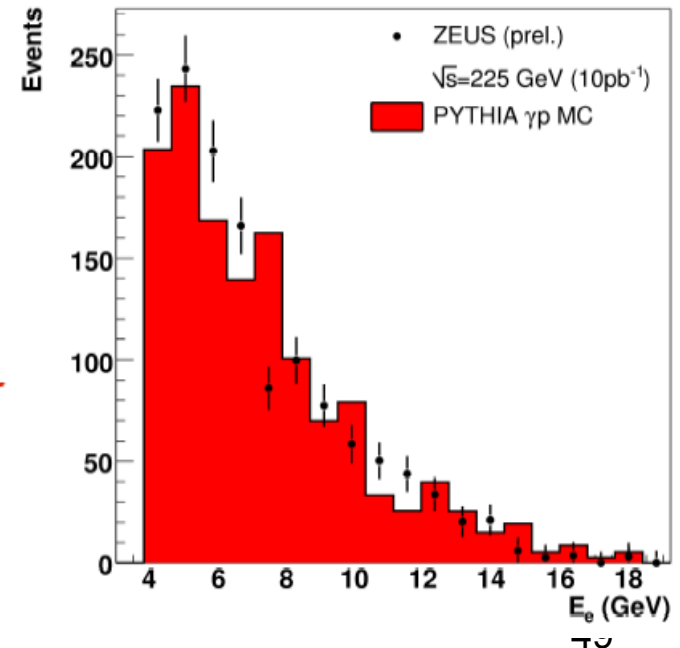
Photoproduction background:

o normalization

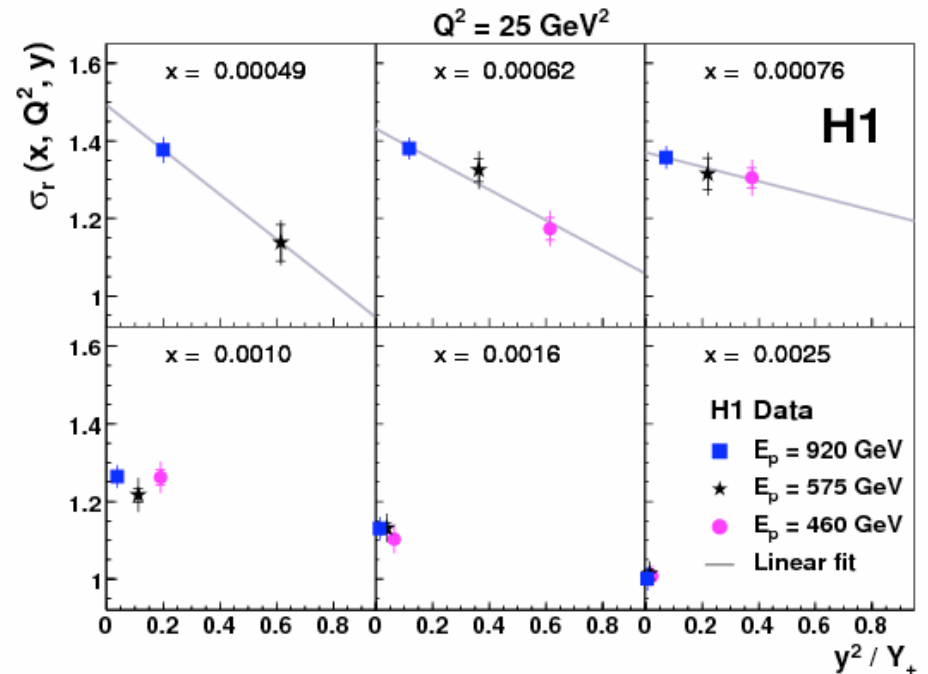
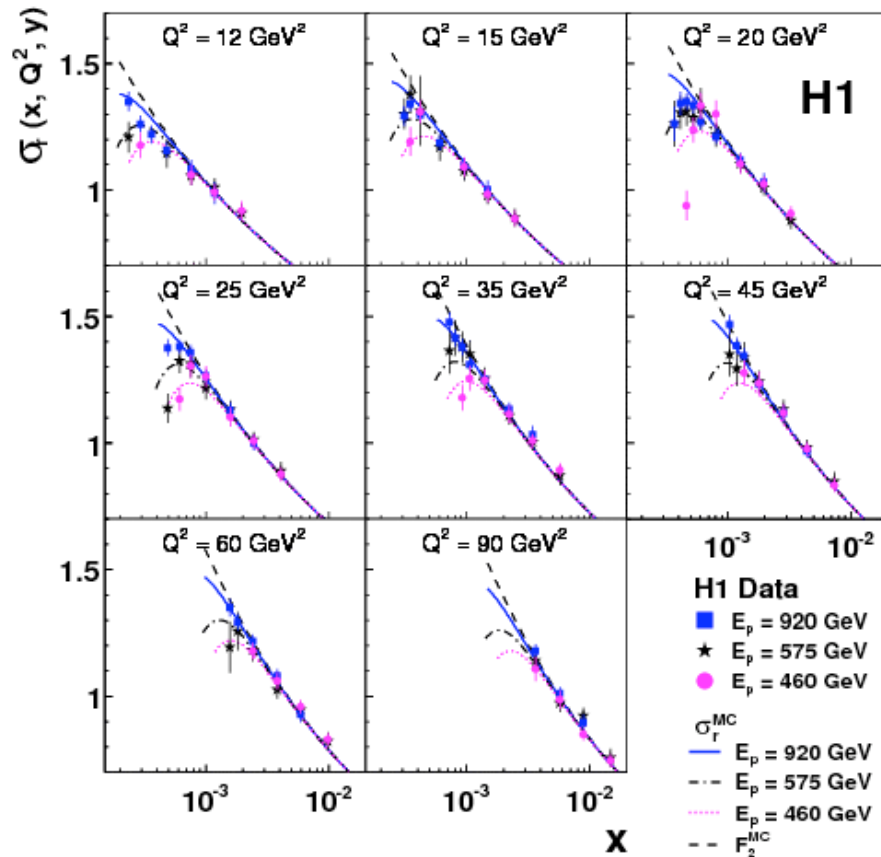
o charged track hits detection at „low“ angle
(from 154° to 168°) to go lower in Q^2 .



ZEUS



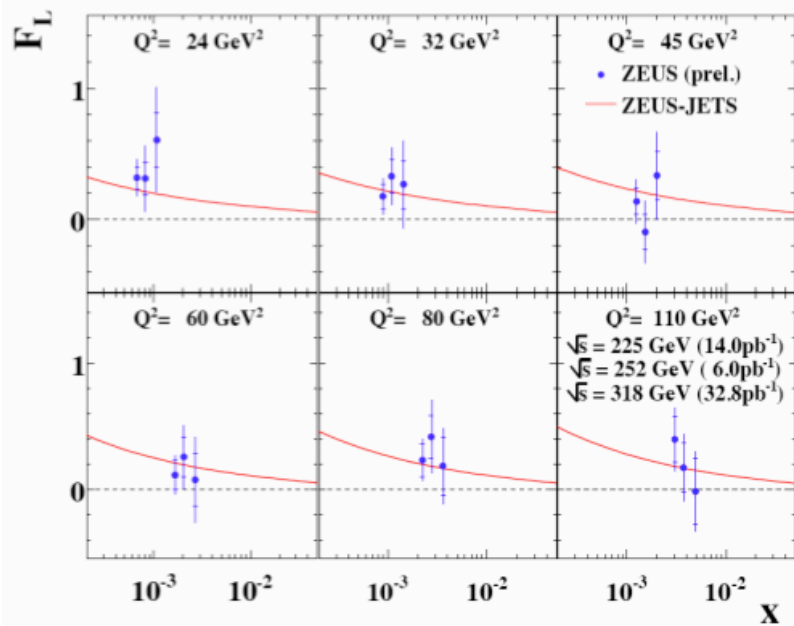
Measurement of F_L



$$\sigma_r = \frac{xQ^4}{2\pi\alpha^2(1+(1-y)^2)} \frac{d^2\sigma(e^\mp p)}{dx dQ^2}$$

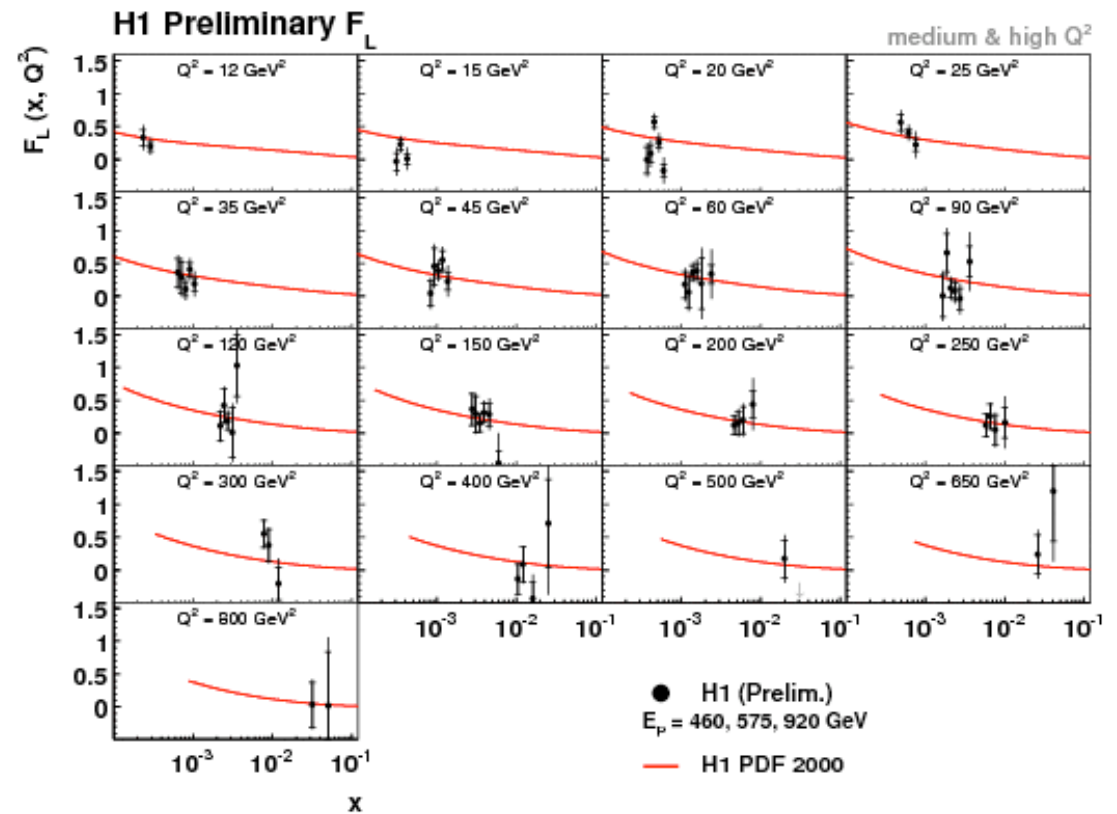
$$\approx \left[F_2 - \frac{y^2}{(1+(1-y)^2)} F_L \right]$$

F_L



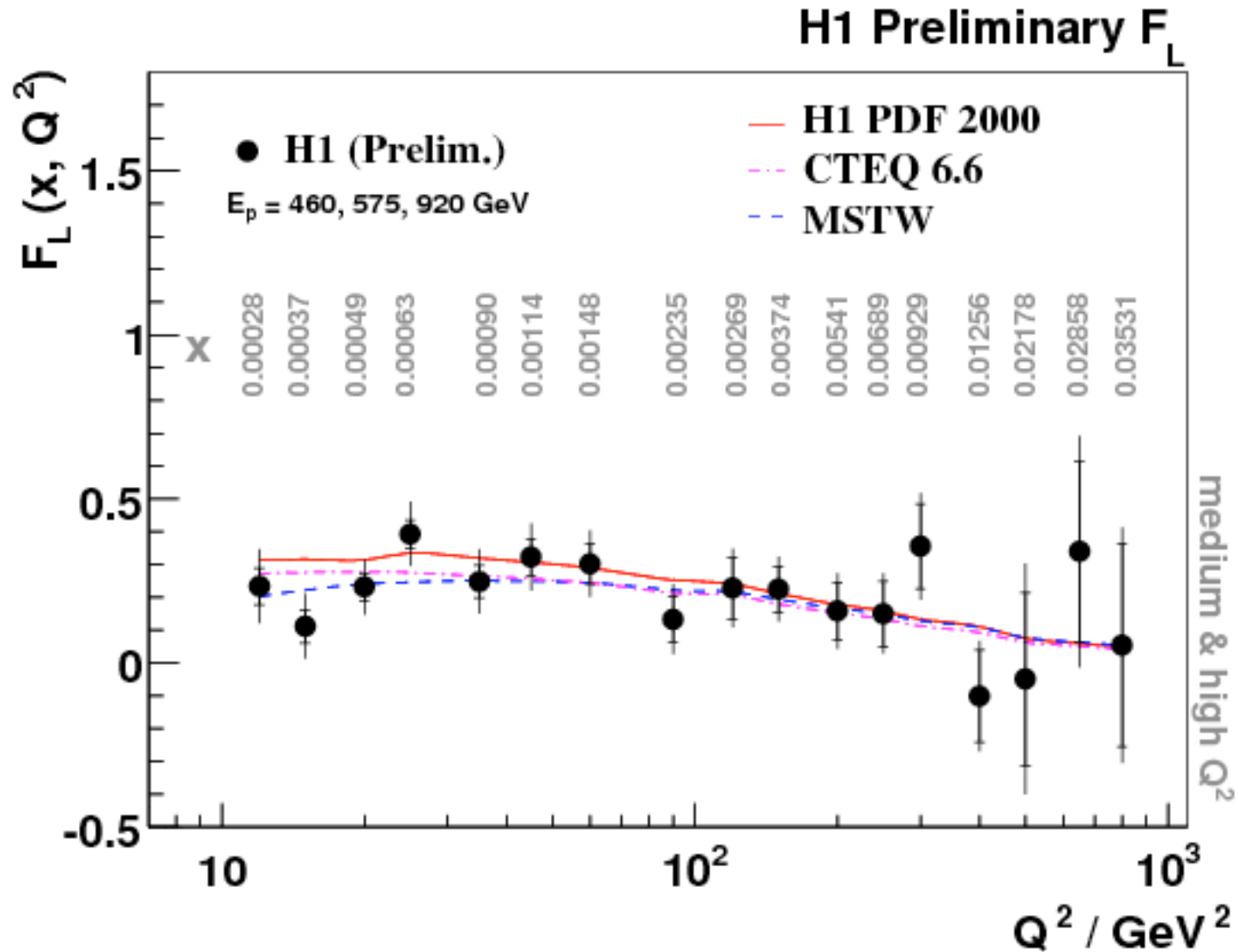
ZEUS, close to publication

H1 (lower Q^2 being looked at)



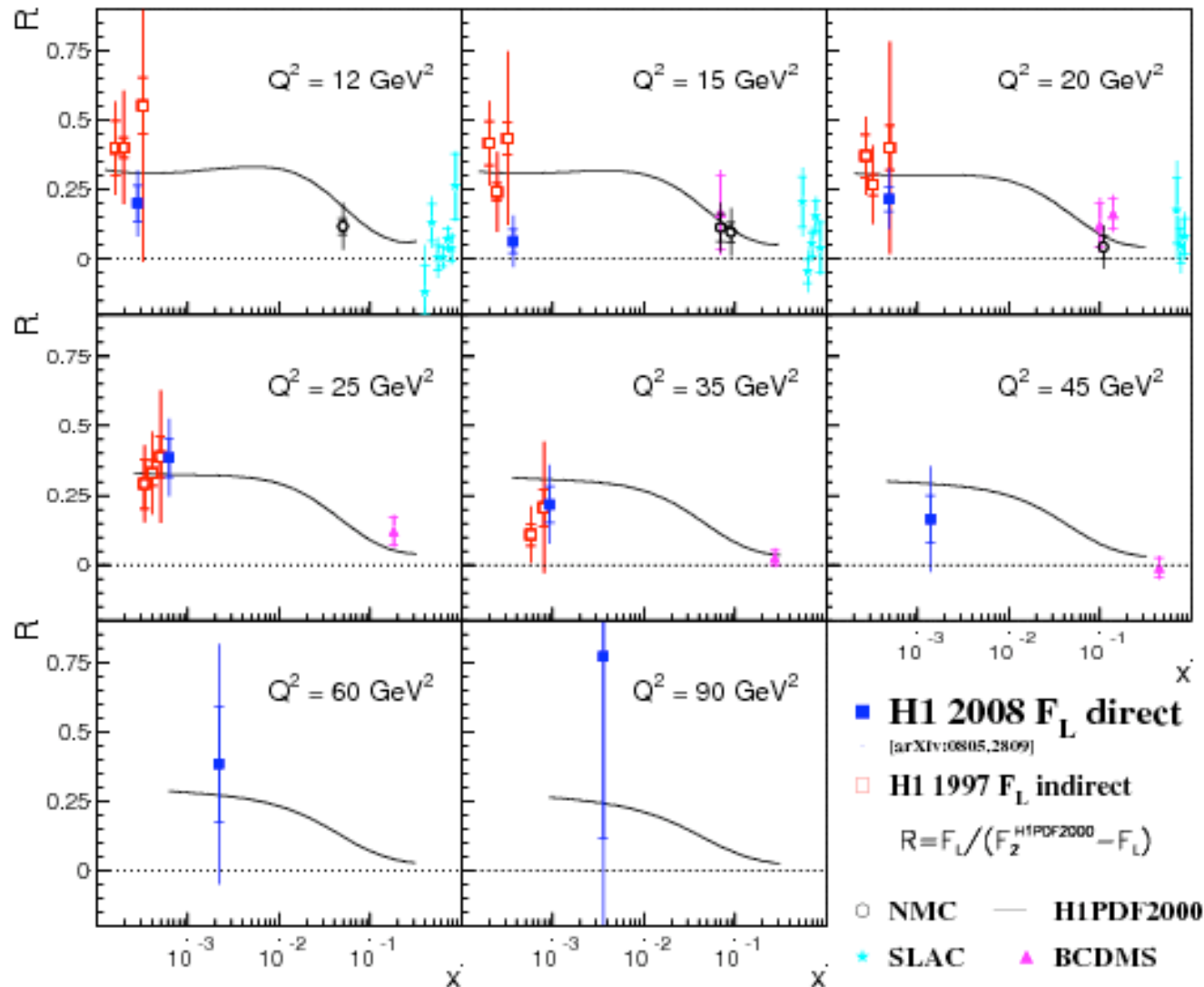
H1 F_L

Comparison to some PDF parametrisations:



H1 F_L

Comparison to previous experiments:



Conclusions

- HERA has provided 15 years of data, still many results to be published.
- Precision test of QCD and parton densities have been performed.
- The publication of combined data will be the main focus.
- The PDF analysis will continue in parallel to the first results of LHC and provide valuable input.
- It was fun at the end to go back to low x and measure F_L .